AD-A172 056 DEVELOPMENT OF VAPOR DISPERSION MODELS FOR NONNEUTRALLY BUOYANT GAS MIXTU..(U) ARKANSAS UNIV FAYETTEVILLE DEPT OF CHEMICAL ENGINEERING T O SPICER ET AL. SEP 86 1/2

UNCLASSIFIED AFESC/ESL-TR-86-24 DTCG23-80-C-2029 F/G 4/1 NL

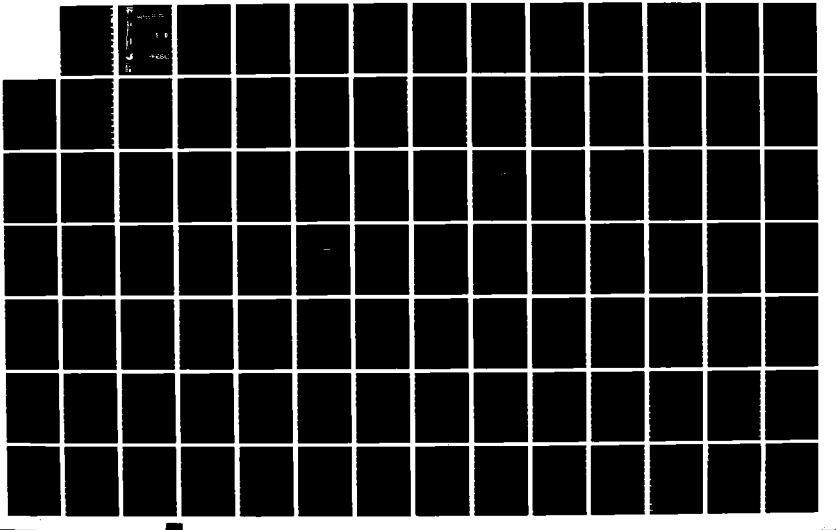

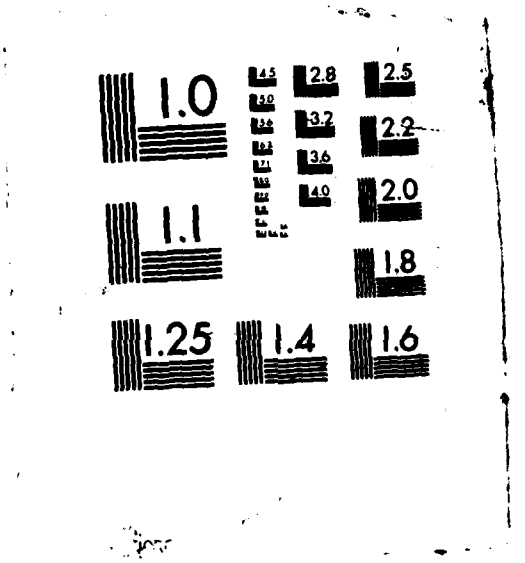
1.0
1.1
1.25
1.4
1.6
2.8
3.2
3.6
4.0
2.5
2.2
2.0
1.8

ESL-TR-86-24

Development of Vapor Dispersion Models for Nonneutrally Buoyant Gas Mixtures--Analysis of USAF/N_2O_4 Test Data

THOMAS O. SPICER
JERRY A. HAVENS

UNIVERSITY OF ARKANSAS CHEMICAL ENGINEERING DEPARTMENT
FAYETTEVILLE, ARKANSAS 72701

SEPTEMBER 1986

FINAL REPORT

FEBRUARY 1985 - JULY 1985

AFESC

ENGINEERING & SERVICES LABORATORY
AIR FORCE ENGINEERING & SERVICES CENTER
TYNDALL AIR FORCE BASE, FLORIDA 32403

NOTICE

PLEASE DO NOT REQUEST COPIES OF THIS REPORT FROM HQ AFESC/RD (ENGINEERING AND SERVICES LABORATORY). ADDITIONAL COPIES MAY BE PURCHASED FROM:

NATIONAL TECHNICAL INFORMATION SERVICE
5285 PORT ROYAL ROAD
SPRINGFIELD, VIRGINIA 22161

FEDERAL GOVERNMENT AGENCIES AND THEIR CONTRACTORS REGISTERED WITH DEFENSE TECHNICAL INFORMATION CENTER SHOULD DIRECT REQUESTS FOR COPIES OF THIS REPORT TO:

DEFENSE TECHNICAL INFORMATION CENTER
CAMERON STATION
ALEXANDRIA, VIRGINIA 22314

UNCLASSIFIED

SECURITY CLASSIFICATION OF THIS PAGE

AD-A172056

REPORT DOCUMENTATION PAGE

1a. REPORT SECURITY CLASSIFICATION: Unclassified	1b. RESTRICTIVE MARKINGS: N/A
2a. SECURITY CLASSIFICATION AUTHORITY: N/A	3. DISTRIBUTION/AVAILABILITY OF REPORT: Approved for public release Distribution unlimited
2b. DECLASSIFICATION/DOWNGRADING SCHEDULE: N/A	
4. PERFORMING ORGANIZATION REPORT NUMBER(S): N/A	5. MONITORING ORGANIZATION REPORT NUMBER(S): ESL-TR-86-24
6a. NAME OF PERFORMING ORGANIZATION: University of Arkansas Chemical Engineering Dept; 6b. OFFICE SYMBOL (If applicable): N/A	7a. NAME OF MONITORING ORGANIZATION: U.S. Air Force Engineering and Services Center
6c. ADDRESS (City, State and ZIP Code): Fayetteville, Arkansas 72701	7b. ADDRESS (City, State and ZIP Code): Air Force Engineering and Services Center/ RDVS Tyndall AFB FL 32403-6001
8a. NAME OF FUNDING/SPONSORING ORGANIZATION: U.S. Air Force; 8b. OFFICE SYMBOL (If applicable): N/A	9. PROCUREMENT INSTRUMENT IDENTIFICATION NUMBER: DTCG23-80-C-20029
8c. ADDRESS (City, State and ZIP Code): U.S. Coast Guard Headquarters 2100 2d St., SW Washington DC 20593	10. SOURCE OF FUNDING NOS.

PROGRAM ELEMENT NO.	PROJECT NO.	TASK NO.	WORK UNIT NO.
N/A	N/A	N/A	N/A

11. TITLE (Include Security Classification): DEVELOPMENT OF VAPOR DISPERSION (Cont'd on reverse)

12. PERSONAL AUTHOR(S): Thomas O. Spicer; Jerry A. Havens

13a. TYPE OF REPORT	13b. TIME COVERED	14. DATE OF REPORT (Yr., Mo., Day)	15. PAGE COUNT
Final	FROM 2/1/85 TO 7/31/85	September 1986	111

16. SUPPLEMENTARY NOTATION: Availability of this report is specified on reverse of front cover.

17. COSATI CODES			18. SUBJECT TERMS (Continue on reverse if necessary and identify by block number)
FIELD	GROUP	SUB. GR.	Dense Gas; DEGADIS; Heavier-Than-Air Gas; Model Evaluation; Dispersion Modeling; Release Richardson Number
09	02		
01	05		

19. ABSTRACT (Continue on reverse if necessary and identify by block number)

Two field-scale releases (Eagle 3 and 6) of nitrogen tetroxide (N_2O_4) performed by the Lawrence Livermore National Laboratory for the U.S. Air Force as part of the Eagle series are examined. An analysis of the chemical interaction of N_2O_4 with the ambient humidity and oxygen is made. The reported source mass evolution rate is adjusted to account for these reactions; the source rate for Eagle 3 is between 2.9 and 3.1 kg/s, while for Eagle 6, the source rate is between 1.6 and 1.7 kg/s. Reported nitrogen dioxide (NO_2) concentrations downwind of the source are adjusted for the source mass evolution rate, and these observed conditions are compared with predicted concentrations using the Ocean Breeze/Dry Gulch model, the Pasquill-Hanna Gaussian plume model, and DEGADIS. (Developed for the U.S. Coast Guard, DEGADIS describes the negative buoyancy-driven flows and reduced vertical mixing observed for releases of heavier-than-air gases in the atmosphere.) Observed Gaussian equivalent concentration profiles (σ_y and σ_z) are also compared to predicted values. For these tests, the DEGADIS predictions are consistent with the observed concentration and values σ_y and σ_z, while the Gaussian plume models are not consistent. (Cont'd on reverse.)

20. DISTRIBUTION/AVAILABILITY OF ABSTRACT	21. ABSTRACT SECURITY CLASSIFICATION
UNCLASSIFIED/UNLIMITED ☒ SAME AS RPT. ☐ DTIC USERS ☐	UNCLASSIFIED

22a. NAME OF RESPONSIBLE INDIVIDUAL	22b. TELEPHONE NUMBER (Include Area Code)	22c. OFFICE SYMBOL
Capt Larry Key	(904) 283-4234	HQ AFESC/RDVS

DD FORM 1473, 83 APR EDITION OF 1 JAN 73 IS OBSOLETE.

UNCLASSIFIED

SECURITY CLASSIFICATION OF THIS PAGE

11. (Cont'd) MODELS FOR NONNEUTRALLY BUOYANT GAS MIXTURES--ANALYSIS OF USAF/N_2O_4 TEST DATA

19. (Cont'd)→Furthermore, the importance of negative buoyancy-driven flows and decreased vertical mixing rates for Eagle 3 and 6 is predicted by a characteristic release Richardson number.

PREFACE

This report was prepared by the Chemical Engineering Department, University of Arkansas, Fayetteville, Arkansas 72701, under Contract Number DTCG23-80-C-20029, for the U.S. Coast Guard Headquarters, Washington DC 20593, and for the Air Force Engineering and Services Center, Engineering and Services Laboratory (AFESC/RDVS), Tyndall Air Force Base, Florida 32403.

This report summarizes work done between 1 February 1985 and 31 July 1985. HQ AFESC/RDVS program manager was Captain Larry Key, and USCG HQ program manager was Lieutenant Commander Peter Tebeau. Dr. Tom McRae of the Lawrence Livermore National Laboratories provided data for the analysis.

This report has been reviewed by the Public Affairs Office (PA) and is releasable to the National Technical Information Service (NTIS) where it will be available to the general public including foreign nationals.

This technical report has been reviewed and is approved for publication.

LAWRENCE E. KEY, Capt, USAF
Project Officer

KENNETH T. DENBLEYKER, Maj, USAF
Chief, Environmental Sciences Branch

ROBERT F. OLFENBUTTEL, Lt Col,USAF,BSC
Chief, Environics Division

JAMES R. VAN ORMAN
Deputy Director of Engineering
and Services Laboratory

(The reverse of this page is blank.)

TABLE OF CONTENTS

Section	Title	Page
I	INTRODUCTION	1
II	CHEMICAL INTERACTION OF N_2O_4 MIXTURES WITH AMBIENT HUMIDITY	4
	A. NEAR-FIELD CHEMICAL INTERACTIONS	5
	B. FAR-FIELD CHEMICAL INTERACTIONS	11
III	ADJUSTED MASS FLUX AND CONCENTRATIONS	13
IV	GAS DISPERSION MODEL COMPARISONS	16
V	RELEASE RICHARDSON NUMBER	22
VI	CONCLUSIONS	26
APPENDIX		
A	DESCRIPTION OF THE DEGADIS DENSE GAS DISPERSION MODEL	29
	REFERENCES	85

LIST OF FIGURES

Figure	Title	Page
1	Schematic Diagram of DEGADIS Dense Gas Dispersion Model	19
A-1	Schematic Diagram of DEGADIS Dense Gas Dispersion Model	31
A-2	Schematic Diagram of a Radially Spreading Cloud	33
A-3	The Unsteady Gravity Current (Reference 23)	35
A-4	The Head of a Steady Gravity Current (References 23 and 26)	38
A-5	Summary of Simulation Definition Input Information for DEGADIS	62
A-6	EAGLE6.INP Listing	66

LIST OF TABLES

Table	Title	Page
1	Summary of Eagle Test Conditions (Reference 2)	3
2	Thermodynamic Properties (Reference 9)	5
3	Summary of Source Rates and Downwind Concentration for Eagle 3 and 6	15
4	Comparison of Eagle 3 and Eagle 6 Test Results and Gas Dispersion Model Predictions	17
A-1	Typical Atmospheric Boundary Layer Stability and Wind Profile Correlations	52
A-2	Typical Values of Surface Roughness	84

LIST OF SYMBOLS

a_v	empirical constant (1.3)
B_{EFF}	effective width of gas plume (m)
B_i'	local half-width of source seen by observer i (m)
b	half-width of horizontally homogeneous central section of gas plume (m)
b_v	empirical constant (1.2)
C_E	constant (1.15) in density intrusion (spreading) relation
$C_{NO_2 i}$	initial concentration of NO_2 ($kmol/m^3$)
$C_{NO_2 f}$	final concentration of NO_2 ($kmol/m^3$)
C_p	heat capacity (J/kg K)
C_{p_a}	heat capacity of ambient humid air
C_{p_c}	heat capacity of contaminant (J/kg K)
C_{p_w}	heat capacity of water (liquid phase) (J/kg K)
C_{NO}	NO concentration ($kmol/m^3$)
C_{O_2}	O_2 concentration ($kmol/m^3$)
c	local concentration (kg/m^3)
c_c	centerline, ground-level concentration (kg/m^3)
$c_{c,L}$	vertically averaged layer concentration (kg/m^3)
c_f	friction coefficient
c_c'	centerline, ground-level concentration corrected for x-direction dispersion (kg/m^3)
D	source diameter (m)
D_h	added enthalpy (J/kg)
$\mathcal{D}$	diffusivity (m^2/s)
d_v	empirical constant (0.64)

E	plume strength (kg/s)
$E(t)$	source rate (kg/s)
e_v	empirical constant (20.)
F	overall mass transfer coefficient (kg/m^2 s)
F_f	mass transfer coefficient due to forced convection (kg/m^2 s)
F_n	mass transfer coefficient due to natural convection (kg/m^2 s)
f	conversion efficiency defined as the kmol of NO_2 reacted per kmol released gas expressed as pure NO_2
Gr	Grashoff number
g	acceleration of gravity (m/s^2)
H	height or depth of density intrusion or cloud (m)
H_a	ambient absolute humidity (kg water/kg dry air)
H_{EFF}	effective cloud depth (m)
H_h	height of head in density-driven flow (m)
H_L	total layer depth (m)
H_t	height of tail in density-driven flow (m)
H_1	average depth of gravity current head (m)
H_4	depth of inward internal flow in a gravity current head (m)
h	enthalpy of source blanket (J/kg)
h_a	enthalpy of ambient humid air (J/kg)
h_E	enthalpy associated with primary source mass rate (J/kg)
h_f	heat transfer coefficient due to forced convection (J/m^2 s K)
h_L	enthalpy of vertically averaged layer (J/kg)
h_n	heat transfer coefficient due to natural convection (J/m^2 s K)

h_0	overall heat transfer coefficient (J/m^2 s K)
h_w	enthalpy associated with mass flux of water from surface (J/kg)
K_0	constant ($m^{1-\gamma_1}$)
$K_{eq,A}$	equilibrium constant for Reaction (A) (NO_2/N_2O_4 equilibrium)
$K_{eq,D}$	equilibrium constant for Reaction (D) (HNO_3 formation)
K_y	horizontal turbulent diffusivity (m^2/s)
K_z	vertical turbulent diffusivity (m^2/s)
K_1	kinetic constant for NO oxidation
k	von Karman's constant, 0.35
k_1	constant
k_2	constant
L	source length (m)
M	total cloud mass (kg)
M_a	total mass of air in the cloud (kg)
M_c	total mass of contaminant in the cloud (kg)
M_i	initial cloud mass (kg)
MW	molecular weight
MW_c	contaminant molecular weight
$\dot{M}_a$	mass rate of air entrainment into the cloud (kg/s)
$\dot{M}_{w,s}$	mass rate of water transfer to the cloud from the water surface under the source (kg/s)
$\dot{m}$	mass source evolution rate (kg/s)
N	number of observers
Nu	Nusselt number
Pr	Prandtl number
P	cloud momentum (kg m/s)

P_h	momentum of head in density-driven flow (kg m/s)
P_t	momentum of tail in density-driven flow (kg m/s)
P_v	virtual momentum due to acceleration reaction (kg m/s)
p	atmospheric pressure (atm)
p_w^*	vapor pressure of water (atm)
p_{NO_2}	partial pressure of NO_2 (atm)
$p_{N_2O_4}$	partial pressure of N_2O_4 (atm)
p_1	model heat capacity constant
Q	volumetric release rate (m^3/s)
Q_E	source mass flux (kg/m^2 s)
Q_e	volumetric entrainment flow (m/s)
Q_1	flux of ambient fluid into front of gravity current head (m/s)
$\dot{Q}_s$	rate of heat transfer from the surface (J/s)
Q_*	atmospheric takeup flux (kg/m^2 s)
Q_{*max}	maximum atmospheric takeup flux of contaminant (kg/m^2 s)
q_s	surface heat flux (J/m^2 s)
q_1	model heat capacity constant
R	gas source cloud radius (m)
R_h	inner radius of head in density-driven flow (m)
R_m	value of R when ($\pi R^2 Q_*$) is a maximum (m)
R_{max}	maximum radius of the cloud (m)
R_p	primary source radius (m)
Ri_T	Richardson number associated with temperature differences
Ri_c	initial Richardson number for continuous release

Ri'_*	Richardson number associated with density differences corrected for convective scale velocity
Ri_*	Richardson number based on the friction velocity
Ri	Richardson number
Sc	Schmidt number
Sh	Sherwood number
St_H	Stanton number for heat transfer
St_M	Stanton number for mass transfer
S_y	horizontal concentration scaling parameter (m)
S_z	vertical concentration scaling parameter (m)
S_{z0}	S_z at the downwind edge of the source ($x = L/2$) (m)
S_{z0_m}	value of S_{z0} when ($\pi R^2 Q_*$) is a maximum (m)
T	gas mixture temperature (K)
$T_{c,L}$	temperature associated with averaged enthalpy (K)
T_s	surface temperature (K)
T_0	contaminant storage temperature
t	time (s)
t_s	specified time (s)
t_{dn_i}	time when observer i encounters downwind edge (s)
t_{up_i}	time when observer i encounters upwind edge (s)
u	average wind velocity (m/s)
u_a	ambient average velocity (m/s)
u_e	horizontal or frontal entrainment velocity (m/s)
u_{EFF}	effective cloud advection velocity (m/s)
u_f	cloud front velocity (m/s)
u_i	velocity of observer i (m/s)

u_L	average transport velocity associated with H_L (m/s)
u_x	wind velocity, along x-direction (m/s)
u_0	wind velocity measured at $z = z_0$ (m/s)
u_3	internal flow out of gravity current head (m/s)
u_4	internal flow into gravity current head (m/s)
u_*	friction velocity (m/s)
$\bar{u}$	characteristic average velocity (m/s)
V_H	heat transfer velocity (0.0125 m/s)
w	ambient absolute humidity
w_a	mass fraction of air
w_c	mass fraction of contaminant
w_e	vertical entrainment velocity associated with H_L (m/s)
w_*	convective scale velocity (m/s)
w'_e	entrainment velocity associated with H_{EFF} (m/s)
w_w	mass of water absorbed on the nitric acid nuclei per mass of nitric acid formed
x_N	mass fraction of NO present due to Reaction (D) or (E)
x_{acid}	mass fraction of nitric acid formed due to Reaction (D) or (E)
x_A	mass fraction of ambient air
$x_i(t)$	x position of observer i at time t (m)
x_{pi}	position of puff center from to observer i (m)
x_s	mass fraction of equilibrium mixture of NO_2/N_2O_4 before reaction
x_t	downwind distance where gravity spreading terminates (m)
x_p	virtual point source distance (m)
x_v	measured mass fraction of the NO_2/N_2O_4 concentration after reaction

x_{dn_i}	x position of downwind edge of source for observer i
x_{up_i}	x position of upwind edge of source for observer i
x_w	mass fraction of ambient humidity (water)
$x_{w,A}$	mass fraction of water absorbed on the nitric acid nuclei
x,y,z	Cartesian coordinates (m)
x_0	downwind edge of the gas source (m)
$\bar{x}_w$	mass fraction of water after nitric acid nuclei reaction and water adsorption on the nitric acid nuclei
x_A	mass fraction of ambient air
y_{H_2O}	H_2O mole fraction
y_{NO_2}	NO_2 mole fraction
$y_{N_2O_4}$	N_2O_4 mole fraction
y_{HNO_3}	HNO_3 mole fraction
y_{NO}	NO mole fraction
y_{NO_2}	NO_2 mole fraction
$y_{NO_2 i}$	initial mole fraction of NO_2
y_v	contaminant mole fraction predicted by OB/DG
z_R	surface roughness (m)
z_0	reference height in wind velocity profile specification (m)
α	constant in power law wind profile
β	constant in σ_y correlation
Γ	gamma function
γ	ratio of $(\rho - \rho_a)/c_c$
γ_1	constant
Δ	ratio of $(\rho - \rho_a)/\rho$

ΔT	temperature driving force (K) $(T_s - T_{c,L})$ or $(T_s - T)$
Δ'	ratio of $(\rho - \rho_a)/\rho_a$
δ	constant in σ_y correlation
δ_L	empirical constant (2.15)
δ_v	constant (0.20)
η	conversion efficiency of nitric acid formation based on the change in NO_2 concentration divided by the initial NO_2 concentration
ϵ	frontal entrainment coefficient (0.59)
ζ	collection of terms $(m^{1(1+a)})$
λ	Monin-Obukhov length (m)
μ	viscosity (kg/m s)
ρ	density of gas air mixture (kg/m^3)
ρ_a	ambient density (kg/m^3)
ρ_c	cloud density (kg/m^3)
ρ_L	vertically averaged layer density (kg/m)
ρ_v	vapor density at ambient temperature and pressure
ρ_a	ambient air density (kg/m^3)
ρ_i	initial gas density (kg/m^3)
ρ_0	density of contaminant's saturated vapor at T_0 (kg/m^3)
σ_x	x-direction dispersion coefficient (m)
σ_y	Pasquill-Gifford lateral dispersion coefficient (m)
σ_z	z-direction dispersion coefficient (m)
ϕ	function describing influence of stable density stratification on vertical diffusion
$\hat{\phi}$	integrated source entrainment function
ψ	logarithmic velocity profile correction function

(The reverse of this page is blank.)

SECTION I

INTRODUCTION

The U.S. Air Force (USAF) is taking steps to improve and update safety procedures available for use during operations involving hazardous chemicals and fuels. In support of this effort, the Lawrence Livermore National Laboratory conducted two field scale releases (Eagle 3 and 6) of nitrogen tetroxide (N_2O_4) at the U.S. Department of Energy (DOE) Nevada Test Site during 1983. The N_2O_4 liquid was released directly on the ground through a circular distribution piping network with six outlets. Although the test site surface is known for water impermeability, N_2O_4 absorbed readily, causing the surface to buckle and heave up several inches. At the completion of each test, nitrogen gas was used to purge the piping system of N_2O_4, thereby enhancing N_2O_4 vaporization. An array of sensors was placed 25 meters downwind of the gas source in order to determine the mass evolution rate of the released gas. Determination of the mass evolution rate was to be accomplished by measurement of the N_2O_4 concentration, temperature, and velocity as the vapor cloud passed through the array. The chemical interaction of N_2O_4 vapor with ambient humidity and oxygen is discussed in Section II. In Section III, a range of source evolution rates is obtained, based on the measured mass rates at 25 meters and the conclusions of Section II. Another array of sensors designed to measure NO_2 concentration, temperature, and velocity was placed 785 meters downwind of the source to measure the concentration and vertical extent of the gas cloud as it moved downwind after release.

Concentration measurements at 785 meters are adjusted for reaction effects based on the measured mass evolution rate. Two of these releases, Eagle 3 and 6, provided sufficient data for comparison and assessment of atmospheric gas dispersion modeling techniques (Reference 1); test conditions for Eagle 3 and 6 are summarized in Table 1.

In his final report, McRae (Reference 1) showed that standard passive dispersion modeling techniques inadequately described the dispersion processes present during Eagle 3 and 6. (N_2O_4 vapor is heavier than air for the same temperature and pressure.) In fact, it is well established that atmospheric dispersion of heavier-than-air gases (HTAGes) may differ importantly from passive dispersion (trace contaminant dispersion). The following phases are used to describe HTAG dispersion in the atmosphere (References 3 and 4):

--negative buoyancy-dominated dispersion

--stably stratified shear flow

--passive dispersion due to atmospheric turbulence

An interactive computer model (DEGADIS) which accounts for these dispersion phases has been developed for the U.S. Coast Guard (Reference 3). Although application of DEGADIS has been primarily directed to the prediction of concentrations in the range of hydrocarbon lower flammability limits (1 to 5 volume percent), an objective of this research is to begin to examine the applicability of DEGADIS to the prediction of concentrations for toxic gases by comparison of DEGADIS predictions with the Eagle series tests.

TABLE 1. SUMMARY OF EAGLE TEST CONDITIONS (Reference 2)

	Eagle 3	Eagle 6
Air temperature at 12 m (^{o}C)	21.9	22.6
Wind speed at 12 m (m/s)	3.66	5.58
Wind variability at 12 m	7.6^{o}	10.8^{o}
Barometric pressure (atm)	0.9079	0.9093
Relative humidity	45%	35%
Reported friction velocity (m/s)	0.081	0.148
Total mass N_2O_4 released (kg)	6090	4930

Section IV compares model predictions to adjusted concentrations and to observed concentration distributions from Eagle 3 and 6. Finally, Section V examines the usefulness of a release Richardson number for determining the relative importance of the three dispersion phases mentioned above.

SECTION II

CHEMICAL INTERACTION OF N_2O_4/NO_2 MIXTURES WITH AMBIENT HUMIDITY

In the liquid phase, N_2O_4/NO_2 mixtures are predominantly N_2O_4; at 1 atm, the concentration of NO_2 in a liquid mixture is less than 0.2 mass percent (Reference 5). In the vapor phase, the equilibrium between N_2O_4 and NO_2 expressed as

$$N_2O_4\ (g) \rightleftharpoons 2NO_2\ (g) \qquad (A)$$

has been extensively investigated (References 6, 7, and 8). Reaction (A) is essentially instantaneous (Reference 5), and the equilibrium constant $K_{eq,A}$ based on ideal gas behavior and the thermodynamic values given in Table 2 is given by

$$K_{eq,A} = \frac{p_{NO_2}^2}{p_{N_2O_4}\ (1\ atm)} = \frac{y_{NO_2}^2}{y_{N_2O_4}}$$

$$= \exp\ [23.48 - 0.3473\ \ln\ (T) - 6983/T] \qquad (1)$$

where p is the partial pressure in atm and y is the mole fraction; T is the mixture absolute temperature (K).

TABLE 2. THERMODYNAMIC PROPERTIES (Reference 9)

	ΔH_f kcal/gmol	ΔG_f kcal/gmole	C_p cal/gmol K
NO (g)	21.57	20.69	7.133
NO_2 (g)	7.93	12.26	8.89
N_2O_4 (g)	2.19	23.38	18.47
HNO_3 (g)	-32.28	-17.87	12.75
HNO_3 (l)	-41.40	-19.10	--
H_2O (g)	-57.796	-54.634	8.025

A. NEAR-FIELD CHEMICAL INTERACTIONS

The LLNL infrared (IR) spectrophotometric sensors used for the 25-meter array in the Eagle series tests measured the transmission through the gas sample over four different frequency bands denoted as Channels M, F, R, and E; Channels E and F are reference channels because no absorption at these frequencies would be caused by the presence of any of the gas species under consideration. Channels M and R were intended to measure the N_2O_4/NO_2 mixture concentration based upon the additional absorption due to N_2O_4 (utilizing the equilibrium relationship between NO_2 and N_2O_4 given above).

Unfortunately, typical IR sensor output during the spill tests indicated essentially the same attenuation in all four channels indicating something other than N_2O_4, NO_2, HNO_3, HNO_2, and ambient atmospheric gases was present. When tested using N_2O_4 from onsite

storage, the IR sensors behaved as expected, showing little attenuation in Channels E and F. Grab samples of the gas cloud from the 25-meter array and N_2O_4 in the spill pipe were analyzed at LLNL by mass and IR spectroscopy; no indication of a foreign gas capable of producing attenuation in all four channels was present. As reported in Reference 2, the attenuation was concluded to be the result of aerosol scattering which would produce broad-band attenuation.

A possible source of the aerosol is from the reaction of ambient humidity with N_2O_4/NO_2 to form nitric acid (HNO_3) which has been extensively studied (References 10, 11, and 12). Aerosol formation is known to take place when the partial pressure of HNO_3 exceeds its vapor pressure at the mixture temperature (i.e., the mixture temperature is below the HNO_3 dew point temperature). England and Corcoran (Reference 10) proposed the following mechanism to describe the reaction of N_2O_4/NO_2 with water vapor when the partial pressure of HNO_3 does not exceed its vapor pressure (estimated to be 50 ppm of HNO_3 at atmospheric pressure and ambient temperatures):

$$N_2O_4\ (g) \rightleftharpoons 2NO_2\ (g) \qquad (A)$$

$$N_2O_4\ (g) + H_2O\ (g) \rightarrow HNO_2\ (g) + HNO_3\ (g) \qquad (B)$$

$$2HNO_2\ (g) \rightarrow NO\ (g) + NO_2\ (g) + H_2O\ (g) \qquad (C)$$

which gives an overall reaction of

$$3NO_2\ (g) + H_2O\ (g) \rightarrow NO\ (g) + 2HNO_3\ (g) \qquad (D)$$

Using Table 2, the equilibrium constant without mist formation is given by

$$K_{eq,D} = \frac{y_{HNO_3}^2 \, y_{NO}}{y_{NO_2}^3 \, y_{H_2O}} = \exp\,[-12.95 - 1.038 \ln T + 4212/T] \qquad (2)$$

When the concentration of HNO_3 exceeds 50 ppm, the gas phase reaction supplies nitric acid nuclei where water vapor readily condenses to form strong nitric acid droplets. The overall reaction is given by

$$3NO_{2(g)} + H_2O_{(g)} \rightarrow NO_{(g)} + 2HNO_{3(aq)} \qquad (E)$$

although the reaction mechanism remains in the gas phase (Reference 11). As Reactions (D) or (E) proceed, the ambient water vapor present acts to reduce the NO_2 concentration, thereby reducing the N_2O_4 quantities, and the mist formed by Reaction (E) further inhibits the measurement of N_2O_4.

Although the mist presence made direct measurement of the total cloud concentration impossible with the sensors which were deployed, McRae et al. (Reference 2) analyzed the IR gas sensor data assuming the attenuation was the same in channels M and F. Under this assumption, reported concentrations apply to the vapor portion of the cloud only. The following development attempts to provide an upper and lower bound of the total cloud concentration based on the observed concentration of the vapor portion of the cloud assuming no reaction takes place. These concentration bounds are compared with the vapor dispersion models in Section IV.

If the gas is considered to be a mixture of air (nitrogen/oxygen mixture) x_A, water (ambient humidity) x_w, and an equilibrium gas phase mixture of NO_2/N_2O_4 x_s without any reaction taking place, the sum of these mass fractions would be

$$x_s + x_w + x_A = x_s + (1 + w)\, x_A = 1. \tag{3}$$

where w is the ambient absolute humidity. Following any reaction, the sum of the mass fractions would be

$$x_v + \bar{x}_w + x_N + x_A + x_{w,A} + x_{acid} = 1. \tag{4}$$

where the mass fraction of the measured NO_2/N_2O_4 mixture is x_v, the unabsorbed and unreacted water is $\bar{x}_w$, the NO present due to reaction is x_N, the water absorbed at the HNO_3 nuclei is $x_{w,A}$, and the HNO_3 present due to reaction is x_{acid}. Equation (4) assumes the mass fraction of air remains unchanged (open to question for longer time scales due to combination of O_2 with NO, and discussed later), and there is little error in the measured NO_2/N_2O_4 concentration. Combining Equations (3) and (4),

$$x_s = x_v + x_N + x_{acid} - (x_w - \bar{x}_w - x_{w,A}) \tag{5}$$

where $(x_w - \bar{x}_w - x_{w,A})$ is the mass of water reacted per mass of mixture. If the stoichiometry of Reactions (D) or (E) holds, the following ratios apply:

$$x_N = \frac{\text{kg NO formed}}{\text{kg mixture}} = \left[\frac{\text{1 kmol NO formed}}{\text{kmol } H_2O \text{ reacted}}\right]\left[\frac{\text{30 kg NO formed}}{\text{kmol NO formed}}\right] * \left[\frac{\text{1 kmol } H_2O \text{ reacted}}{\text{18 kg } H_2O \text{ reacted}}\right]\left[\frac{\text{kg } H_2O \text{ reacted}}{\text{kg mixture}}\right]$$

and

$$x_{acid} = \frac{\text{kg } HNO_3 \text{ formed}}{\text{kg mixture}} = \left[\frac{\text{2 kmol } HNO_3 \text{ formed}}{\text{kmol } H_2O \text{ reacted}}\right] \left[\frac{\text{63 kg } HNO_3 \text{ formed}}{\text{kmol } HNO_3 \text{ formed}}\right] * \left[\frac{\text{1 kmol } H_2O \text{ reacted}}{\text{18 kg } H_2O \text{ reacted}}\right] \left[\frac{\text{kg } H_2O \text{ reacted}}{\text{kg mixture}}\right]$$

Using these ratios,

$$x_s = x_v + 7.67\ (x_w - \bar{x}_w - x_{w,A}) \qquad (6)$$

Although Reaction (E) has been shown to be fast (References 11 and 12), the reaction has not been shown to go to completion. If a conversion efficiency f is defined as

$$f = \frac{\text{kmol } NO_2 \text{ reacted}}{\text{kmol } NO_2 \text{ without reaction}}$$

where the (kmol NO_2 without reaction) is the quantity of NO_2/N_2O_4 without any reaction taking place and expressed as pure NO_2, the mass of water reacted per mass of mixture is given by:

$$(x_w - \bar{x}_w - x_{w,A}) = \frac{\text{kg } H_2O \text{ reacted}}{\text{kg mixture}}$$

$$= \left[\frac{\text{18 kg } H_2O \text{ reacted}}{\text{kmol } H_2O \text{ reacted}}\right] \left[\frac{\text{kmol } H_2O \text{ reacted}}{\text{3 kmol } NO_2 \text{ reacted}}\right] * \left[\frac{\text{kmol } NO_2 \text{ reacted}}{\text{kmol } NO_2 \text{ without reaction}}\right] * \left[\frac{\text{kmol } NO_2 \text{ without reaction}}{\text{kg mixture}}\right]$$

$$= 6f \left[\frac{\text{kmol } NO_2 \text{ without reaction}}{\text{kg } NO_2/N_2O_4 \text{ without reaction}}\right] * \left[\frac{\text{kg } NO_2/N_2O_4 \text{ without reaction}}{\text{kg mixture}}\right]$$

But, the second term in brackets is x_s while the first term is (1/46). Or,

$$(x_w - \bar{x}_w - x_{w,A}) = \frac{6}{46} f x_s$$

which with Equation (6) gives

$$x_s = x_v/(1 - f) \tag{7}$$

Although Equation (7) becomes indeterminant when f = 1, this does not indicate a problem since if f = 1, x_v would be 0. It should be noted that f will be less than 1 if water is the limiting reactant in Reaction (E). Furthermore, no assumption about which reactant may be limiting has been used to derive Equation (7).

Goyer (Reference 11) measured the extent of Reaction (E) by mixing humid air with a dry nitrogen stream which had been bubbled through liquid N_2O_4; NO_2 gas concentrations were measured photometrically, and a conversion efficiency η was defined as

$$\eta = \frac{C_{NO_2 i} - C_{NO_2 f}}{C_{NO_2 i}}$$

where $C_{NO_2 i}$ is the initial NO_2 concentration (kmol NO_2/m^3) and $C_{NO_2 f}$ is the final NO_2 concentration. Using Goyer's data (Reference 11), $\eta < 0.07$ for the conditions of Eagle 3 and Eagle 6. It can be shown that

$$f = \eta/(1. + 2y_{NO_2 i}/K_{eq,A})$$

where $y_{NO_2 i}$ is the initial mole fraction of NO_2. Since $f < \eta < 0.07$, use f = 0.07 as an upper bound of the extent of reaction. Or,

$$x_v \leq x_s \leq 1.07\ x_v \tag{8}$$

depending on the actual value of f.

B. FAR-FIELD CHEMICAL INTERACTIONS

In addition to the previously mentioned reactions, NO may be oxidized to NO_2 by the reaction

$$2NO + O_2 \rightarrow 2NO_2 \tag{F}$$

Although Reaction (F) is suspected to be unimportant at the 25-meter sensor array, it may be important for the 785-meter sensor array since it will theoretically go to completion. Burdick (Reference 13) investigated Reaction (F) and found the kinetics to be described by

$$-\frac{dC_{NO}}{dt} = K_1\ C_{O_2} C_{NO}^2$$

with the value of $K_1 = 1.2 \times 10^4\ l^2/gmol^2 s$ at 25°C. Using the maximum possible concentration of NO_2/N_2O_4 at the 25-meter array and assuming the concentration of oxygen is essentially constant, the minimum value of (C_{NO}/C_{NO_i}) can be estimated to be about 0.40 for Eagle 3 and 0.52 for Eagle 6. Although Reaction (F) generates NO_2 at the expense of NO, this will force more HNO_3 to be generated due to the equilibrium constraints of the faster Reaction (D) (at the expense of NO_2). The net effect of Reaction (F) is thought to be small.

Although Goyer (Reference 11) observed the rapid evaporation of nitric acid mist formed for relative humidities below about 20

percent, the evaporation process is believed to be much slower due to the higher humidity of Eagle 3 and 6. It should be noted that the first HNO_3 damage to the low level IR sensors at the 25-meter array occurred after Eagle 3; Eagle 3 was the first test with a relative humidity much greater than 20 percent. Since Goyer's experiments (Reference 11) were carried out with air, any decomposition of HNO_3 to NO_2 would be taken into account with the observed reaction extent (including any decomposition acceleration due to the presence of NO). For the data of the 785-meter array, the same mass fraction range in Equation (8) is assumed to apply to each of the measured concentrations.

SECTION III

ADJUSTED MASS FLUX AND CONCENTRATION

The array of sensors placed 25 meters downwind of the gas source was designed to measure the N_2O_4 concentration, temperature, and velocity of the gas cloud as it moved downwind. From these measurements, the mass rate of gas ($\dot{m}$) 25 meters downwind of the source is given by

$$\dot{m} = \int_A \rho x_s u dA$$

where ρ is the mixture density and u is the measured velocity. With a steady-state release, the mass rate of gas passing a plane 25 meters downwind of the source is also the mass evolution rate of gas from the source. Note that the mass flux of gas is based on NO_2/N_2O_4 concentrations without any reaction taking place.

The concentration range from Equation (8) can be used to adjust the measured vapor flux at the 25-meter array. Using the (Reference 1) measured vapor evolution rate of NO_2/N_2O_4 for Eagle 3 and 6 (McRae, 1985) and Equation (8), the mass evolution rate for Eagle 3 ranged between 2.9 and 3.1 kg/s (170 kg/min and 190 kg/min) while the mass evolution rate for Eagle 6 ranged between 1.6 and 1.7 kg/s (97 kg/min and 103 kg/min). These ranges of the source evolution rate are consistent with the observed extensive outgassing times for both Eagle 3 and 6. McRae (Reference 1) reported that 100 to 1000 gallons of water were sprayed on the release area to dilute the N_2O_4 absorbed into the ground so that acceptable vapor concentration levels would be realized. Based on these evolution rates, 78 to 80

percent of the N_2O_4 released for both Eagle 3 and Eagle 6 absorbed into the soil at the source during the test, in agreement with previous small scale tests at Edwards Air Force Base (Reference 14). (This agreement may not be significant due to the differences in the soil between the Eagle and Edwards tests.)

In addition to the measured NO_2 concentration at 785 meters shown in Table 3, the following method was used as another estimate of the NO_2 concentration at 785 meters. For each of the Eagle tests reported by McRae (Reference 1), an appropriate steady source time period was chosen for each experiment, taking into account ambient wind velocities and directions over the travel time between the source and the 785-meter array. After choosing this time, the observed concentration contours were adjusted to a Gaussian equivalent cross section. These cross sections were integrated to determine the observed mass flux of NO_2/N_2O_4 through the array. Since a steady-state experiment must observe the same mass flux between the 25-meter array and the 785-meter array, a maximum centerline concentration may be calculated assuming the observed profiles (σ_x and σ_y values) to be applicable. The results of these calculations are summarized in Table 3. All of the reported concentrations are in equivalent concentration of NO_2 ($y_{NO_2} + 2y_{N_2O_4}$), and for these concentration ranges at 785 meters, $y_{NO_2} >> y_{N_2O_4}$. The overall NO_2 concentration range in Table 3 represents the minimum and maximum NO_2 concentrations from all indications for the steady state NO_2 concentration at 785 meters for Eagle 3 and 6.

TABLE 3. SUMMARY OF SOURCE RATES AND DOWNWIND CONCENTRATIONS FOR EAGLE 3 AND 6

	Eagle 3	Eagle 6
Mass rate range of unreacted NO_2/N_2O_4 at 25 meters (kg/s)	2.9-3.1	1.6-1.7
Total mass of NO_2/N_2O_4 passing 25-meter array (kg)	1200-1300	970-1030
Observed Gaussian equivalent distribution at 785 meters		
σ_y (crosswind)*	35 m	35 m
σ_z (vertical)*	3.8 m	7.6 m
Observed maximum NO_2 concentration at 785 meters (ppm)*	500	315
Observed maximum NO_2 concentration at 785 meters taking reaction into account (ppm)	535	340
Range of maximum NO_2 concentration at 785 meters based on mass flux at 25 meters (ppm)	970-1040	160-170
Overall NO_2 concentration range at 785 meters (ppm)	500-1040	160-340

*Reference 1

SECTION IV

GAS DISPERSION MODEL COMPARISONS

McRae (Reference 1) compared several Gaussian-profile model predictions to the measured downwind NO_2 concentration as well as the equivalent Gaussian cross-section profiles observed in the experiments. Two passive dispersion models (Ocean Breeze/Dry Gulch and Pasquill-Hanna) are compared to the data presented in Section III. Also, comparisons are made to the DEGADIS model developed for the U.S. Coast Guard (Reference 3).

The Ocean Breeze/Dry Gulch (OB/DG) model is the product of two experimental programs involving the release and measurement of a trace atmospheric contaminant. The results were correlated to a simple empirical model (Reference 15). The same procedures used by McRae (Reference 1) were used for calculating the wind field variation (σ_θ) and the characteristic temperature difference (ΔT). Although the OB/DG model predicts the concentration at 1.5 meters elevation, the difference between this elevation and the sensor elevation of 1.0 meters would not be great. The OB/DG results for Eagle 3 and 6 are listed in Table 4.

TABLE 4. COMPARISON OF EAGLE 3 AND EAGLE 6 TEST RESULTS AND GAS DISPERSION MODEL PREDICTIONS

	Maximum NO_2 Concentration Range (ppm)*	σy (m)	σz (m)
EAGLE 3			
Test Results	500-1040	35	3.8
OB/DG	68-73	--	--
Gaussian Plume	68-73	60.5	31.9
DEGADIS	880-1170	57.6-60.7**	2.3-2.9***
EAGLE 6			
Test Results	160-340	35	7.6
OB/DG	20-21	--	--
Gaussian Plume	25-27	60.5	31.9
DEGADIS	190-220	55.6-56.6**	4.5-4.9***

*The concentration range for the model predictions are for the estimated source evolution rate range.

**calculated as $S_y/\sqrt{2}$

***calculated as $S_z/\sqrt{2}$

The Pasquill-Hanna Gaussian plume model has proven to be applicable to atmospheric dispersion problems when the dispersion of the contaminant is only a function of the atmospheric turbulence and the plume does not perturb the ambient flow field. The steady Gaussian plume model for ground level releases is given by

$$y_v = \frac{\dot{m}}{\pi \rho_v \sigma_y \sigma_z u} \exp \left[- \left(\frac{y}{\sqrt{2}\ \sigma_y} \right)^2 - \left(\frac{z}{\sqrt{2}\ \sigma_z} \right)^2 \right] \qquad (10)$$

where y_v is the contaminant mole fraction, $\dot{m}$ is the source evolution rate, ρ_v is the vapor density at ambient temperature and pressure, u is the average wind speed, and σ_y and σ_z determine the shape of the Gaussian profile taken from Hanna et al. (Reference 16). The same procedures used by McRae (Reference 1) were used in determining the parameters in Equation (10). The model results for Eagle 3 and 6 are listed in Table 4.

The DEGADIS (DEnse GAs DISpersion) model is an adaptation of the Shell HEGADAS model described by Colenbrander (Reference 17) and Colenbrander and Puttock (Reference 18). The near-field, buoyancy-dominated regime is modeled using a lumped parameter model of a heavier-than-air gas (HTAG) "secondary source" cloud which incorporates air entrainment at the gravity-spreading front using a frontal entrainment velocity. The downwind dispersion phase of the calculation assumes a power law concentration distribution in the vertical direction and a modified Gaussian profile in the horizontal direction with a power law specification for the wind profile (Figure 1). A description of the DEGADIS model is included in Appendix A. The source model represents a spatially averaged concentration of gas present over the primary source, while the downwind dispersion phase of the calculation models an ensemble average of the concentration downwind of the source. The vertical

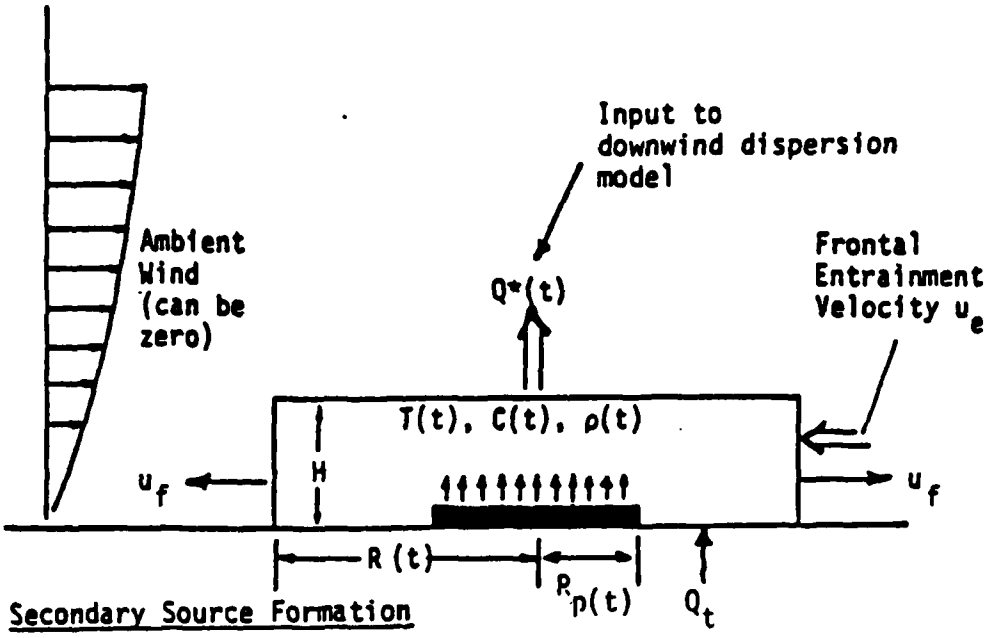

Secondary Source Formation

$$c(x,y,z) = c_c(x) \exp\left[-\left(\frac{|y|-b(x)}{S_y(x)}\right)^2 - \left(\frac{z}{S_z(x)}\right)^{1+a}\right], |y| > b$$

$$c(x,y,z) = c_c(x) \exp\left[-\left(\frac{z}{S_z(x)}\right)^{1+a}\right], |y| \le b$$

$$u_x = u_0\left(\frac{z}{z_0}\right)^a$$

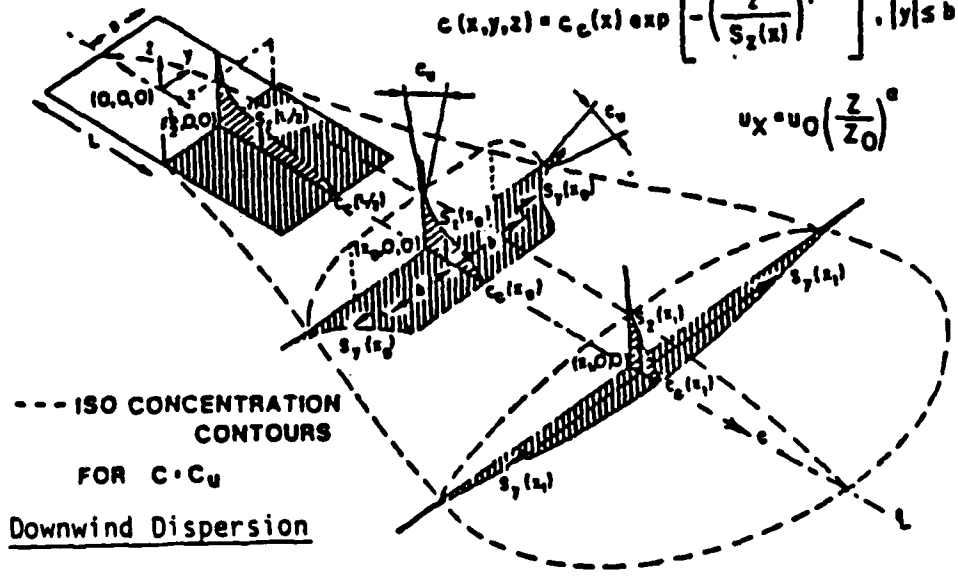

--- ISO CONCENTRATION CONTOURS FOR $C = C_u$

Downwind Dispersion

Figure 1. Schematic Diagram of DEGADIS Dense Gas Dispersion Model

mixing rate is based on laboratory-scale data for vertical mixing in stably density-stratified fluids reported by Kantha et al. (Reference 19), Lofquist (Reference 20), and McQuaid (Reference 21). The vertical dispersion parameter S_z and the horizontal dispersion parameter S_y determine the vertical and horizontal profiles, respectively. The rates of change of S_y and S_z approach the rates of change of σ_y and σ_z, respectively, as the density of the plume approaches the ambient air density.

Because several parameters are calculated from the Pasquill stability class and the surface roughness, DEGADIS requires no more atmospheric information than the Pasquill-Hanna Gaussian plume model. However, because of the dependence of the vertical dispersion rate on the gas mixture density, the gas mixture density must be specified as a function of concentration. For locations near the source, the gas mixture is predominantly N_2O_4, while for distances far from the source, the gas mixture is predominantly NO_2. Two simulations were made to bound the behavior of the reacting gas mixture as it moved downwind. For one bounding simulation, the contaminant gas was assumed to be pure NO_2 at the temperature of the liquid pool ($-7^{\circ}C$ for Eagle 3 and $15^{\circ}C$ for Eagle 6). For the other bounding simulation, the contaminant gas was assumed to be pure N_2O_4 at the temperature of the liquid pool; under these conditions, the predicted N_2O_4 mole fraction was multiplied by 2 for the equivalent NO_2 mole fraction. For these bounding simulations, the calculations were performed assuming no reaction took place

(since any reaction which would occur would cause the gas mixture density to fall between the bounds of NO_2 without reaction and N_2O_4 without reaction). The DEGADIS simulation results for Eagle 3 and 6 are presented in Table 4. The ranges of NO_2 concentration, σ_y, and σ_z represent the minimum and maximum variable values calculated using the source evolution rate range and both of the bounding density specifications.

For Eagle 3 and 6, the passive dispersion models tend to underpredict the maximum concentration because of an overprediction of the vertical mixing rate (i.e., the predicted σ_z is greater than the observed σ_z). On the other hand, DEGADIS predicts maximum centerline concentrations and similarity distribution parameters σ_y and σ_z which are consistent with the experimental data; closer agreement of DEGADIS-predicted values of σ_z with observed values of σ_z compared to the passive Gaussian plume models is attributed to correctly predicting the decreased vertical mixing rate for the initial phase of the release.

SECTION V

RELEASE RICHARDSON NUMBER

The fact that passive dispersion prediction techniques may be inadequate for releases of N_2O_4 might be anticipated because N_2O_4 vapor is heavier than air for the same temperature and pressure. Passive dispersion prediction techniques are based on the assumption that the dispersing contaminant does not disturb the ambient flow field. In contrast, the dispersion phases of a heavier-than-air gas (HTAG) may also include negative buoyancy-dominated dispersion and stably stratified shear flow as well as passive dispersion (References 3 and 4). The negative buoyancy-dominated dispersion phase is characterized by turbulent flow structures (for example, the classic "gravity current") which result in rapid mixing. Between these two extremes, the stably stratified shear flow phase is characterized by vertical mixing rates which are lower than the passive dispersion phase, and the turbulent structures in the negative buoyancy-dominated dispersion phase are generally no longer significant.

Notice, however, that these dispersion phases are not governed only by the density of the dispersing gas but also by other conditions. Consider the release of a gas slightly heavier than air in a very light wind; such a release could exhibit the characteristics of the negative buoyancy-dominated dispersion phase even though the contaminant is only slightly heavier than air. Furthermore, consider a small release of gas which is several times heavier than air in high winds; such a

release could be controlled by the ambient wind field (passive dispersion) even though the contaminant is several times heavier than air. Therefore, the question of whether a release is dominated by "dense gas effects" is governed by three factors, including the density of the released gas, the rate of release, and the ambient flow field. (A release is said to be dominated by "dense gas effects" if the maximum concentration or the concentration distribution at the concentration of interest is significantly affected by the negative buoyancy-dominated dispersion phase and/or the stably stratified shear flow phase.)

These qualitative characteristics can be quantitatively predicted by the release Richardson number

$$Ri_c = \frac{g}{u_*^2}\left(\frac{\rho_i - \rho_a}{\rho_a}\right)\left(\frac{\dot{m}}{\rho_i u D}\right)$$

where ρ_i is the initial (source) gas density. This Richardson number represents a ratio of the characteristic potential energy of the gas release to a measure of the ambient turbulent kinetic energy. When the characteristic potential energy of the release is much greater than the ambient turbulent kinetic energy ($Ri_c >> 1$), the negative buoyancy-dominated dispersion phase predominates near the source. As the gas moves downwind and dilutes, the dispersion is next controlled by the stably stratified shear flow phase, and as the gas is further diluted, the dispersion is then passive. In contrast, when the characteristic potential energy of the gas release is much less

than the ambient turbulent kinetic energy ($Ri_c < 1$), the passive dispersion phase predominates near the source. Based on experimental work reported by Britter (References 22 and 23), three release Richardson number ranges roughly correspond to the three dispersion phases discussed above, namely:

$Ri_c \gtrsim 32$	negative buoyancy-dominated dispersion
$1 \lesssim Ri_c \lesssim 32$	stably stratified shear flow
$Ri_c \lesssim 1$	passive dispersion

where the intermediate range is a transition zone between the two extremes.

For Eagle 3 and 6, ρ_i was calculated, based on an equilibrium mixture of NO_2/N_2O_4 at the liquid pool temperature. Using this definition, $Ri_c \doteq 40$ for Eagle 3 and $Ri_c \doteq 4$ for Eagle 6. (The Eagle 6 Ri_c is lower than the Eagle 3 Ri_c because Eagle 6 had a lower release rate and a higher wind speed than Eagle 6.) From these Richardson numbers, the dispersion in Eagle 3 and 6 would be expected to be inadequately described by passive dispersion prediction techniques such as OB/DG and the Pasquill-Hanna Gaussian plume model; this conclusion is consistent with comparisons of the range of observed maximum concentrations and the similarity distribution parameters σ_y and σ_z with the OB/DG and Pasquill-Hanna Gaussian plume model predictions. In contrast, since DEGADIS was designed to include the three dispersion phases of a HTAG, the dispersion present in Eagle 3 and 6 would be expected to be adequately described by DEGADIS.

Indeed, as indicated in Section IV, the DEGADIS predictions are consistent with the range of observed maximum concentrations and the parameters σ_y and σ_z for Eagle 3 and 6. Reference 3 contains further comparison of DEGADIS with other field tests. (If $Ri_c < 1$, the predictions of the Pasquill-Hanna Gaussian plume model and DEGADIS would be expected to be consistent between themselves as well as with field-scale data (Reference 3).)

SECTION VI

CONCLUSIONS

Two field-scale releases of N_2O_4 (Eagle 3 and 6) performed by the Lawrence Livermore National Laboratory for the U.S. Air Force as part of the Eagle series were examined.

An analysis of the chemical interaction of N_2O_4 with ambient humidity and oxygen was made. Based on this analysis, the source mass evolution rate $\dot{m}$ for Eagle 3 was estimated to be 2.9 kg/s $\leq \dot{m} \leq$ 3.1 kg/s and 1.6 kg/s $\leq \dot{m} \leq$ 1.7 kg/s for Eagle 6. Based on these mass evolution rates, approximately 80 percent of the N_2O_4 released in Eagle 3 and 6 was absorbed into the ground at the spill site.

Observed downwind concentrations and Gaussian equivalent concentration profiles (σ_y and σ_z) were compared to model predictions using the Ocean Breeze/Dry Gulch model (OB/DG), the Pasquill-Hanna Gaussian plume model, and DEGADIS. OB/DG and the Pasquill-Hanna model generally underpredicted the concentration due to an overprediction of the vertical mixing present. On the other hand, DEGADIS predictions were consistent with observed concentrations and profile parameters σ_y and σ_z, indicating the importance of density stratification in these tests.

The importance of density stratification in atmospheric dispersion can be predicted by analyzing a release Richardson number Ri_c. A heavier-than-air gas (HTAG) release is dominated by "dense gas effects" for $Ri_c \gtrsim 1$, but the release will be passive from the source for $Ri_c \lesssim 1$. (A HTAG release is said to be dominated by dense gas effects if the maximum concentration

or the concentration distribution at the concentration of interest is significantly affected by the negative buoyancy-dominated dispersion phase or the stably stratified shear flow phase.) For Eagle 3 and 6, $Ri_c \geq 1$ which indicates that passive dispersion prediction techniques could inadequately predict the dispersion processes present in these tests; this conclusion was substantiated by comparison of test results with OB/DG and the Pasquill-Hanna model as mentioned above. In contrast, DEGADIS, which accounts for the negative buoyancy-dominated phase and the stably stratified shear flow phase as well as the passive dispersion phase, predicted maximum concentrations and distribution parameters which were consistent with observed values.

(The reverse of this page is blank.)

APPENDIX A

DESCRIPTION OF THE
DEGADIS DENSE GAS DISPERSION MODEL

This appendix is a self-contained document with its own format as well as internally consistent numbering system for equations and figures.

DESCRIPTION OF THE
DEGADIS DENSE GAS DISPERSION MODEL

The DEGADIS (DEnse GAs DISpersion) model was developed from research sponsored by the U.S. Coast Guard and the Gas Research Institute (Reference 3). DEGADIS is an adaptation of the Shell HEGADAS model described by Colenbrander (Reference 17) and Colenbrander and Puttock (Reference 18). DEGADIS also incorporates some techniques used by van Ulden (Reference 23).

If the primary source (gas) release rate exceeds the maximum atmospheric takeup rate, a heavier-than-air (HTAG) blanket is formed over the primary source. This near-field, buoyancy-dominated regime is modeled using a lumped parameter model of a HTAG "secondary source" cloud which incorporates air entrainment at the gravity-spreading front using a frontal entrainment velocity. If the primary source release rate does not exceed the maximum atmospheric takeup rate, the released gas is taken up directly by the atmosphere and dispersed downwind. For either source condition, the downwind dispersion phase of the calculation assumes a power law concentration distribution in the vertical direction and a modified Gaussian profile in the horizontal direction with a power law specification for the wind profile (Figure A-1). The source model represents a spatially averaged concentration of gas present over the primary source, while the downwind dispersion phase of the calculation models an ensemble average of the concentration downwind of the source.

A. HEAVIER-THAN-AIR GAS (HTAG) SOURCE CLOUD FORMATION

A lumped parameter model of the formation of the HTAG source cloud or blanket, which may be formed from a primary source such as an evaporating liquid pool or otherwise specified ground level

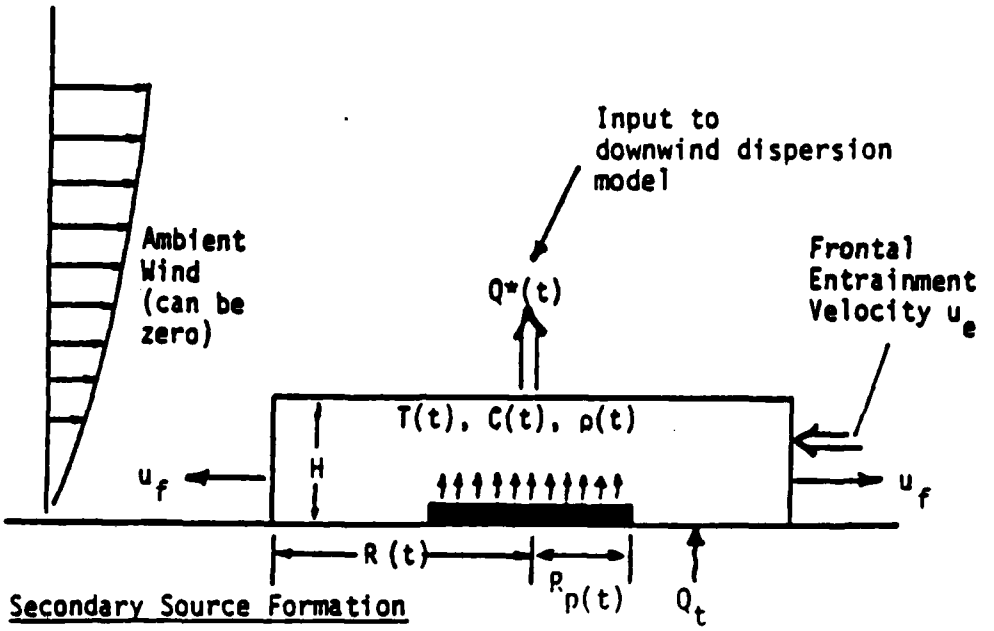

$$c(x,y,z) = c_c(x)\exp\left[-\left(\frac{|y|-b(x)}{S_y(x)}\right)^2-\left(\frac{z}{S_z(x)}\right)^{1+a}\right], |y| > b$$

$$c(x,y,z) = c_c(x)\exp\left[-\left(\frac{z}{S_z(x)}\right)^{1+a}\right], |y| \le b$$

$$u_x = u_0\left(\frac{z}{z_0}\right)^a$$

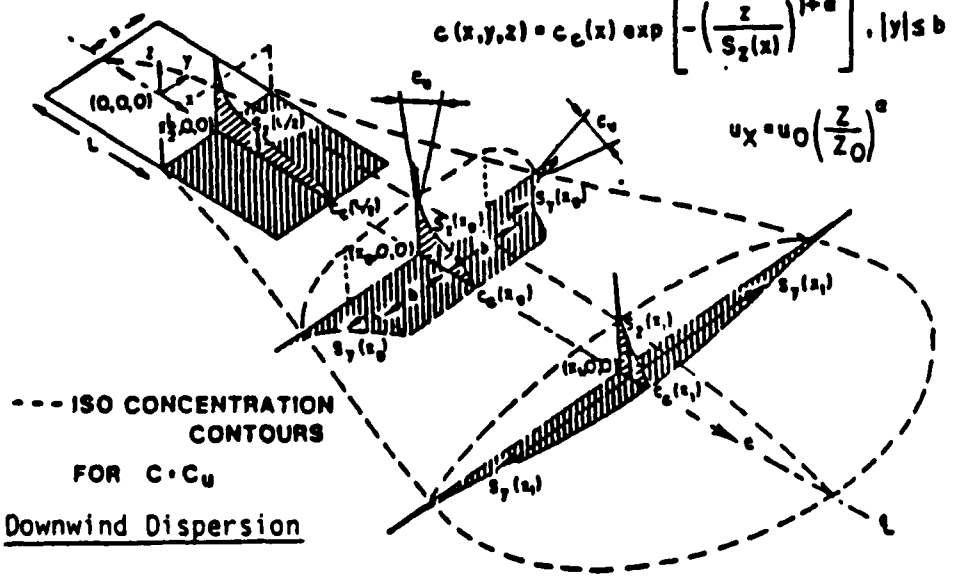

Figure A-1. Schematic diagram of DEGADIS Dense Gas Dispersion Model

emission source, or by an initially specified gas volume of prescribed dimensions for an instantaneous release, is illustrated in Figure A-1. The gas blanket is represented as a cylindrical gas volume which spreads laterally as a density-driven flow with entrainment from the top of the source blanket by wind shear and air entrainment into the advancing front edge. The source blanket will continue to grow over the primary source until the atmospheric takeup rate from the top is matched by the air entrainment rate from the side and, if applicable, by the rate of gas addition from under the blanket. Of course, the blanket is not formed if the atmospheric takeup rate is greater than the evolution rate of the primary source. For application of the downwind calculation procedure, the blanket is modeled as being stationary over the center of the source (x = 0).

1. SECONDARY SOURCE BLANKET EXTENT FOR GROUND LEVEL RELEASES

If a HTAG blanket is present, the (downwind) emission rate from the blanket is equal to the maximum atmospheric takeup rate. That is, for $E(t)/\pi R_p^2(t) > Q_{*_{max}}$, a source blanket is formed over the primary source. The blanket frontal (spreading) velocity is modeled as

$$u_f = C_E \sqrt{g\left(\frac{\rho - \rho_a}{\rho_a}\right) H} \qquad \text{(A-1)}$$

where ρ is the average density of the source blanket. This gravity intrusion relationship is applicable only for $\rho > \rho_a$; the value of C_E used is 1.15 based on laboratory measurements of cloud spreading velocity (Reference 3).

The blanket radius, R, as a function of time is determined by integrating $dR/dt = u_f$. For ground level sources, the blanket spreading is stopped ($dR/dt = 0$) when the total mass of the cloud is decreasing with time. The radius of the blanket is constrained to

be greater than or equal to the radius R_p of any primary (liquid) source present.

2. SECONDARY SOURCE BLANKET EXTENT FOR INSTANTANEOUS RELEASES

The gravity intrusion relationship (Equation (A-1)) will overpredict initial velocities for instantaneous, aboveground releases of a HTAG since no initial acceleration phase is included. In this case, the following procedure adapted from van Ulden (Reference 23) is recommended.

For instantaneous gas releases, the radially symmetric cloud is considered to be composed of a tail section with height H_t and radius R_h and a head section with height H_h (Figure A-2). A momentum

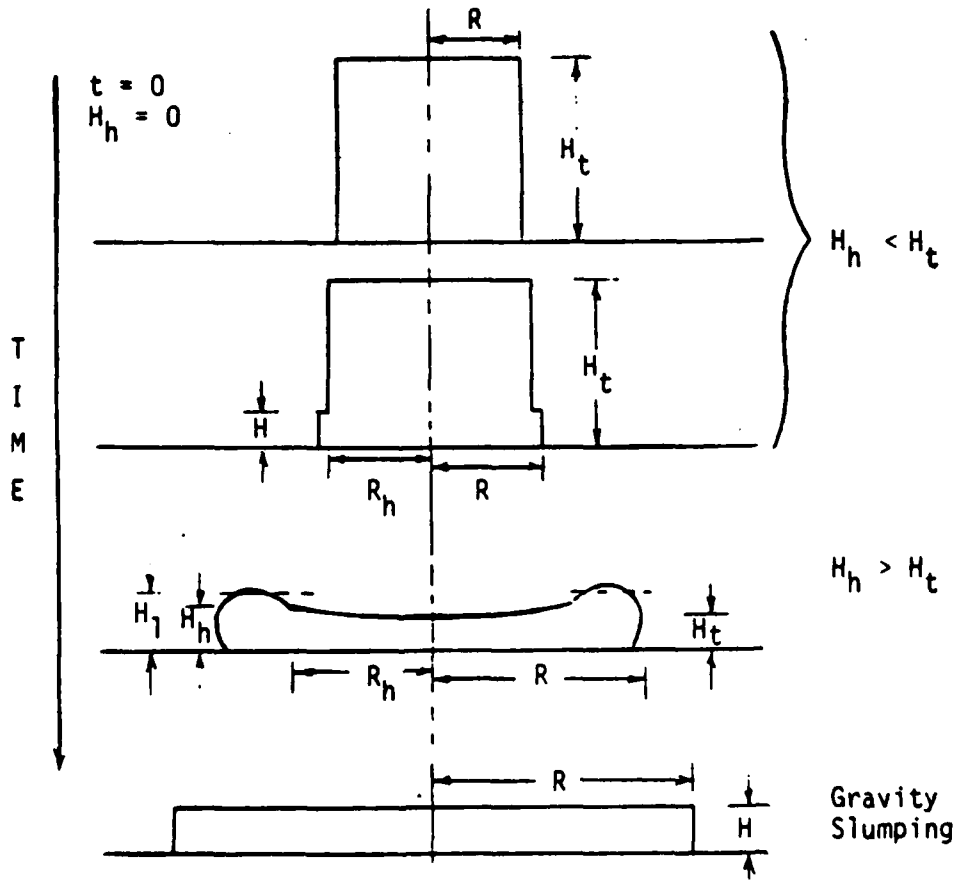

Figure A-2. Schematic Diagram of a Radially Spreading Cloud.

balance is used to account for the acceleration of the cloud from rest; the effect of ambient (wind) momentum is ignored. Although the following equations are derived assuming the primary source rate is zero, the resulting equations are assumed to model the secondary source cloud development when the primary source rate is nonzero. When the frontal velocity from the momentum balance is the same as Equation (A-1), the momentum balance is no longer applied and the frontal velocity is given by Equation (A-1).

There are three main forces acting on the cloud: a static pressure force (F_p), a dynamic drag force (F_d), and a force which accounts for the acceleration reaction of the ambient fluid, represented as a rate of virtual momentum change with respect to time ($-dP_v/dt$). Denoting the momentum of the head and tail as P_h and P_t respectively, the momentum balance is

$$\frac{dP}{dt} = \frac{d}{dt}(P_h + P_t) = F_p + F_d - \frac{dP_v}{dt} \qquad \text{(A-2)}$$

or

$$\frac{d}{dt}(P_h + P_t + P_v) = F_p + F_d \qquad \text{(A-3)}$$

The terms in the momentum balance are evaluated differently for early times before a gravity current head has developed ($H_h < H_t$) and for times after the head has developed but the cloud is still accelerating (Figure A-2). Because the gravity current head develops so rapidly, the model equations describing the times after the gravity current head forms ($H_h \geq H_t$) are derived first. The model equations describing earlier times ($H_h < H_t$) use simplifications of the equations for $H_h \geq H_t$.

a. Unsteady Gravity Current

When the cloud accelerates to the point that $H_h \geq H_t$ (Figures A-2, A-3), the frontal velocity is determined from the momentum balance (Equation (A-2)) as follows.

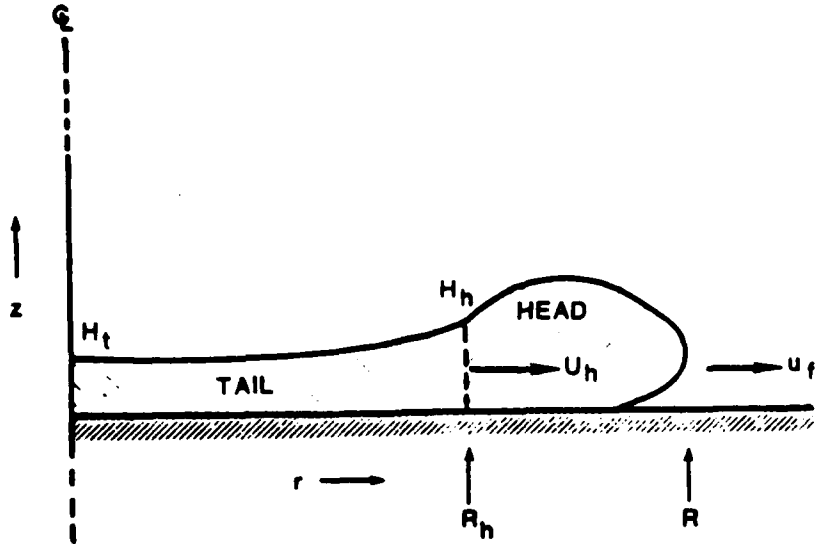

Figure A-3. The Unsteady Gravity Current (Reference 23).

The static pressure force, obtained by integrating the static pressure over the boundary of the current, is

$$F_p = \left(\frac{1}{2} g\Delta\rho H_t \right) \left(2\pi R H_t \right) = \pi g \Delta\rho R H_t^2 \qquad \text{(A-4)}$$

Neglecting the shear stress at the bottom, the dynamic force on the current is the sum of the drag force on the head of the current and the lift force that arises due to asymmetry in the ambient flow around the head. The drag force is represented by

$$F_D = - \frac{d_v}{2} \rho_a u_f^2 \left(2\pi R_h a_v H_h \right) = -a_v d_v \pi R H_h \rho_a u_f^2 \qquad \text{(A-5)}$$

where d_v is an effective drag coefficient and the constant a_v is an empirical ratio of the average head depth H_1 to H_h ($a_v = H_1/H_h$).

The horizontal acceleration reaction ($-dP_v/dt$) is approximated by the reaction to an accelerating elliptical cylinder with an aspect ratio H/R (Reference 24):

$$-\left.\frac{dP_v}{dt}\right|_R = -\frac{d}{dt}\left(k_1 \rho_a \pi R H^2 u_f \right) \tag{A-6}$$

and the vertical acceleration reaction is represented as

$$-\left.\frac{dP_v}{dt}\right|_z = -\frac{d}{dt}\left(k_2 \rho_a \pi R H^2 u_f \right) \tag{A-7}$$

where k_1 and k_2 are coefficients of order one. Using a single constant, Equations (A-6) and (A-7) give

$$-\frac{dP_v}{dt} = -e_v \pi \rho_a \frac{d(RH^2 u_f)}{dt} \tag{A-8}$$

Using Equations (A-4), (A-5), and (A-8), the momentum balance (Equation (A-2)) becomes

$$\frac{dP}{dt} = \pi g \Delta\rho R H_t^2 - a_v d_v \pi \rho_a R H_h u_f^2 - e_v \pi \rho_a \frac{d(RH^2 u_f)}{dt} \tag{A-9}$$

Following van Ulden (References 23, 25), it is assumed that the potential energy decrease due to slumping of the cloud is offset by the production of kinetic energy, which through the action of shear, is partly transformed to turbulent kinetic energy. Part of the turbulent kinetic energy is transformed back into potential energy due to entrainment of air by the cloud. This "buoyant destruction" of kinetic energy is assumed to be proportional to the rate of production of turbulent kinetic energy, and following Simpson and Britter (Reference 26) it is assumed that the turbulent kinetic energy production rate scales as $\pi \rho_a H R u_f^3$. Then,

$$\frac{1}{2} g \Delta\rho H \frac{dV}{dt} = \epsilon \pi \rho_a H R u_f^3 \tag{A-10}$$

which can be written

$$\frac{dV}{dt} = \frac{\epsilon(2\pi RH)u_f}{\left[\frac{g\Delta\rho H}{\rho_a u_f^2}\right]} = \frac{\epsilon(2\pi RH)u_f}{Ri} \tag{A-11}$$

where ϵ is an empirically determined coefficient. Noting dV/dt represents the air entrainment rate,

$$\frac{\dot{M}_a}{\rho_a} = \epsilon(2\pi RH)u_f \Big/ \left[\frac{g\Delta\rho H}{\rho_a u_f^2}\right] \tag{A-12}$$

where $\dot{M}_a$ represents the air entrainment mass rate.

The volume integral

$$V = 2\pi \int_0^R h(r,t)rdr \tag{A-13}$$

where h(r,t) is to be expressed in terms of H_h and H_t, and the momentum integral

$$P = 2\pi \int_0^R \rho u(r,t)h(r,t)rdr = P_t + P_h \tag{A-14}$$

are then approximated with separate analyses of the head and tail of the current.

In the tail of the current, the shallow water equations are assumed applicable. It is assumed that the shape of the current is quasi-stationary in time, and the layer-averaged density difference is assumed horizontally uniform. It follows that the volume and momentum of the tail are given by

$$V_t = \pi R_h^2 \left(H_t + H_h \right) / 2. \tag{A-15}$$

$$P_t = \frac{2}{5} \rho \left(\frac{2}{3} H_t + H_h \right) \pi R_h^3 \frac{u_f}{R} \tag{A-16}$$

A momentum balance for the head region, Figure A-4, assuming quasi-steady state, indicates that the static and dynamic pressure forces on the head should be balanced by the net flux of momentum due to flow into and out of the head. The static pressure and drag are, respectively

$$F_P = \left(\frac{1}{2} g\Delta\rho H_h \right) \left(2\pi R_h H_h \right) = \pi g \Delta\rho R_h H_h^2 \qquad \text{(A-17)}$$

$$F_D = - d_v \left(\frac{1}{2} \rho_a u_f^2 \right) \left[2\pi R_h (a_v H_h) \right]$$

$$= - a_v d_v \rho_a u_f^2 \pi R_h H_h \qquad \text{(A-18)}$$

Near the surface, the inward flow (u_4 in Figure A-4) carries momentum into the head, while the return flow (u_3 in Figure A-4) carries momentum out of the head. Assuming $u_3 \simeq u_4$, $H_4 \simeq 1/2\ H_h$, and $u_4 \simeq \delta_v u_f$, the momentum flux into the head is approximately

$$Q_h \simeq \delta_v^2 \rho_a u_f^2 \left[2\pi R_h H_h \right] \qquad \text{(A-19)}$$

Figure A-4. The head of a steady gravity current (References 26, 23).

Upon rearranging, the momentum balance on the head gives

$$\frac{\rho_a u_f^2}{g\Delta\rho H_h} = 1./\left(d_v a_v - 2\delta_v^2 \right)$$

$$= C_E^2 \qquad \text{(A-20)}$$

when $\delta_v = 0.2$ and $d_v = 0.64$; Equation (A-20) then specifies the head velocity boundary condition. The volume of the head is determined by assuming that the head length scales with H_1. It follows that

$$R - R_h = b_v H_1 \qquad \text{(A-21)}$$

where b_v is an empirical constant, and the volume of the head becomes

$$V_h = \pi a_v b_v (R + R_h) H_h^2 \qquad \text{(A-22)}$$

If the layer-averaged velocity is assumed to increase linearly with r, it follows that

$$u_h = u_f \left(\frac{R_h}{R} \right) \qquad \text{(A-23)}$$

and

$$P_h = \frac{2\pi}{3} \rho a_v \frac{u_f H_h}{R} \left[R^3 - R_h^3 \right] \qquad \text{(A-24)}$$

Along with the definition of u_f,

$$\frac{dR}{dt} = u_f, \qquad \text{(A-25)}$$

Equations (A-9), (A-11), (A-20), (A-21), (A-23), and (A-25) are solved to determine ρ, H_t, H_h, V, P_h, ad P_t ahen $H_h > H_t$.

The constants a_v, b_v, d_v, e_v, and ϵ are assigned values 1.3, 1.0, 0.64, 20., and 0.59, respectively, based on analysis of the still-air HTAG release experiments of Havens and Spicer (Reference 3).

b. Initial Gravity Current Development

To model the initial cloud shape, the tail and head height are considered constant with respect to radius. The momentum balance on the cloud is then given by

$$\frac{d}{dt}\left[P_h + P_t \right] = \pi g \Delta\rho \left[R_h H_t^2 + a_v b_v H_h^3 \right] - \pi a_v d_v \rho_a R H_h u_f^2 - \frac{dP_v}{dt} \qquad \text{(A-26)}$$

where the first term on the right-hand side represents the static pressure force on the head and the second term represents the drag force on the bottom surface of the cloud. The third force is the acceleration reaction by the ambient fluid, represented by Equation (A-8).

The dimensions of the head are again given by

$$R_h = R - a_v b_v H_h \qquad \text{(A-27)}$$

and

$$H_h = \left(\frac{u_f}{C_E} \right)^2 \Big/ [g\Delta\rho/\rho_a] \qquad \text{(A-28)}$$

When the height of the tail H_t is assumed uniform with respect to radius, it follows that

$$H_t = \left[\frac{M}{\rho} - \pi a_v^2 b_v (R + R_h) H_h^2 \right] \Big/ (\pi R_h^2) \qquad \text{(A-29)}$$

where M is the total mass of the cloud. The momentum of the head P_h and tail P_t are then

$$P_h = \frac{2}{3} \pi a_v \frac{\rho H_h (R^3 - R_h^3)}{R} u_f \qquad \text{(A-30)}$$

and

$$P_t = \frac{2}{3}\pi \frac{\rho H_t R_h^3}{R} u_f \qquad \text{(A-31)}$$

Equations (A-26) through (A-31) determine the momentum of the blanket as a function of time, and thus the frontal velocity u_f. The cloud accelerates from rest because $H_h = 0$ initially.

3. Material and Energy Balances

The balance on the total mass of gas in the source blanket ($M = \pi R^2 H\rho$) is

$$\frac{dM}{dt} = \frac{d}{dt}\left[\pi R^2 H\rho\right] = E(t) + \dot{M}_a + \dot{M}_{w,s} - \left(\frac{Q_{*max}}{w_c}\right)\left(\pi R^2\right) \qquad \text{(A-32)}$$

where E(t) is the gas evolution rate from the primary (liquid) source. For spills over water, the water entrainment term ($\dot{M}_{w,s}$) is included in the source blanket description and is calculated from Equation (A-46), and the (humid) air entrainment rate (Equation (A-12)) is

$$\dot{M}_a = 2\pi RH(\epsilon u_f)\rho_a \Big/ \left(g\Delta\rho H/(\rho_a u_f^2)\right) \qquad \text{(A-33)}$$

The balance on the mass of contaminant in the source blanket ($M_c = w_c \pi R^2 H\rho$) is

$$\frac{dM_c}{dt} = \frac{d}{dt}\left[w_c \pi R^2 H\rho\right] = E(t) - Q_{*max}\,(\pi R^2) \qquad \text{(A-34)}$$

and the mass balance on the air in the source blanket ($M_a = w_a \pi R^2 H\rho$) is

$$\frac{dM_a}{dt} = \frac{d}{dt}\left[w_a \pi R^2 H\rho\right] = \frac{\dot{M}_a}{1 + H_a} - \left(\frac{Q_{*max}}{w_c}\right) w_a\,(\pi R^2) \qquad \text{(A-35)}$$

where the ambient humidity is H_a and the mass fraction of contaminant and air are $w_c = M_c/M$ and $w_a = M_a/M$, respectively.

The energy balance on the source blanket ($h\pi R^2 H\rho$) gives

$$\frac{d}{dt}\left[h\pi R^2 H\rho \right] = h_E E(t) + h_a \dot{M}_a + h_w \dot{M}_{w,s} - h\left[\frac{Q_{*max}}{w_c} \right](\pi R^2) + \dot{Q}_s \qquad \text{(A-36)}$$

where h_E is the enthalpy of the emitted gas, h_a is the enthalpy of the ambient humid air, and h_w is the enthalpy of any water vapor entrained by the blanket if over water. There are three alternate submodels included for the heat transfer ($\dot{Q}_s$) from the surface to the cloud.

The simplest method for calculating the heat transfer between the substrate and the gas cloud is to specify a constant heat transfer coefficient for the heat transfer relation

$$\dot{Q}_s = q_s\left[\pi\left(R^2 - R_p^2 \right) \right] = h_0 \Delta T\left[\pi\left(R^2 - R_p^2 \right) \right] \qquad \text{(A-37)}$$

where $\dot{Q}_s$ is the rate of heat transfer to the cloud, q_s is the heat flux, and ΔT is the temperature difference. For the calculation of heat transfer over the source, the temperature difference is based on the average temperature of the blanket.

In the evaluation of the Burro and Coyote series of experiments, Koopman et al. (Reference 27) proposed the following empirical heat transfer coefficient relationship for heat transfer between a cold LNG cloud and the ground

$$h_0 = V_H \rho C_p \qquad \text{(A-38)}$$

where the value of V_H was estimated to be 0.0125 m/s. This constant can be varied in the model.

From the heat transfer coefficient descriptions for heat transfer from a flat plate, the following relationships can be applied. For natural convection, the heat transfer coefficient is estimated using the Nusselt (Nu), Grashoff (Gr) and Prandtl (Pr) numbers, McAdams (Reference 28), from

$$Nu = 0.14\ (Gr\ Pr)^{1/3} \tag{A-39}$$

Or

$$h_n = 0.14 \left[\frac{g\rho^2 C_p^3 \mu}{T\ Pr^2}\ \Delta T \right]^{1/3} \tag{A-40}$$

where h_n is the heat transfer coefficient due to natural convection and Pr is the Prandtl number. In order to simplify the calculations, the parameter group

$$\left[Pr^{-2} \left(C_p MW \right)^3 \left(\frac{\mu}{MW\ T} \right) \right]^{1/3} \tag{A-41}$$

is estimated to be 60 in mks units. The actual value of the group is 47.25, 58.5, and 73.4 for air, methane, and propane, respectively. Equation (A-40) becomes

$$h_n = 18 \left[\left(\frac{\rho}{MW} \right)^2 \Delta T \right]^{1/3} \tag{A-42}$$

where the density ρ, molecular weight MW, and temperature difference ΔT are based on the average composition of the gas blanket.

For forced convection, the Colburn analogy (Reference 29) is applied to a flat plate using the Stanton number for heat transfer St_H and the Prandtl number as

$$St_H\ Pr^{2/3} = \frac{c_f}{2} = \left(\frac{u_*}{\bar{u}} \right)^2 \tag{A-43}$$

Or,

$$h_f = (\bar{u}\rho C_p)\ Pr^{-2/3} \left(\frac{u_*}{\bar{u}} \right)^2 \tag{A-44}$$

where h_f is the heat transfer coefficient due to forced convection. If the velocity is evaluated at the top of the gas blanket and Pr is estimated to be 0.741,

$$h_f = \left[1.22 \frac{u_*^2}{u_0} \left(\frac{z_0}{H} \right)^{\alpha} \right] \rho C_p \qquad \text{(A-45)}$$

The overall heat transfer coefficient is then the maximum of the forced and natural coefficients, i.e. $h_0 = \max(h_f, h_n)$. The heat flux and transfer rate are then estimated by Equation (A-37).

If the gas blanket is formed over water, water will be transferred from the surface to the cloud by a partial pressure driving force associated with the temperature difference between the surface and the gas blanket. The rate of mass transfer of water is

$$\dot{M}_{w,s} = \frac{F_0}{p} \left(p^*_{w,s} - p^*_{w,c} \right) \left[\pi \left(R^2 - R_p^2 \right) \right] \qquad \text{(A-46)}$$

where F_0 is the overall mass transfer coefficient. The driving force is the difference of the vapor pressure of water at the surface temperature $p^*_{w,s}$ and the vapor pressure of water at the cloud temperature $p^*_{w,c}$. The natural convection coefficient is based on the heat transfer coefficient and the analogy between the Sherwood number (Sh) and the Nusselt number (Nu) suggested by Bird et al. (Reference 30)

$$Sh = 0.14 \, (Gr \, Sc)^{1/3} = \frac{F_n L}{\mathcal{D}} \left(\frac{MW}{\rho} \right) \qquad \text{(A-47)}$$

If the Schmidt number is taken as 0.6, and $\left(\frac{\mu}{T \, MW} \right)$ is estimated to be 2.2×10^{-9} in mks units,

$$F_n = 9.9 \times 10^{-3} \left[\left(\frac{\rho}{MW} \right)^2 \Delta T \right]^{1/3} \qquad \text{(A-48)}$$

For forced convection, Treybal (Reference 29) suggests that the Stanton number for mass transfer St_M and the Stanton number for heat transfer St_H are related by

$$St_M = St_H \left(\frac{Pr}{Sc} \right)^{2/3} = 1.15\ St_H \qquad \text{(A-49)}$$

Or,

$$F_f = \frac{20.7\ h_0}{MW\ C_p} \qquad \text{(A-50)}$$

The overall mass transfer coefficient F_0 is calculated as the larger of the natural and forced convection coefficients.

For the case when the primary (liquid) source emission rate E(t) is larger than the atmospheric takeup rate $Q_{*max}\pi R_p^2$, Equations (A-32), (A-34), (A-35), and (A-36) are integrated for the mass, concentration, and enthalpy of the gas blanket along with an appropriate equation of state (i.e., relationship between enthalpy and temperature and between temperature and density).

For the case when the emission rate is not sufficient to form a gas blanket, the flux of contaminant is not determined by the maximum atmospheric takeup rate. Consider the boundary layer formed by the emission of gas into the atmosphere above the primary source. If the source is modeled to have a uniform width 2b and entrain no air along the sides of the layer, the balance on the total material ($\rho_L u_L H_L$) in a differential slice of the layer is

$$\frac{d}{dx}\left[\rho_L u_L H_L \right] = \rho_a w_e + \left(\frac{Q_*}{w_c} \right) \qquad \text{(A-51)}$$

where w_e is the vertical rate of air entrainment into the layer given by Equation (A-83), ρ_L is the average density of the slice, and Q_*/w_c is the total flux of gas from the primary (liquid) source. The balance on the mass flow rate of contaminant ($w_c \rho_L u_L H_L$) at any ($x - x_{up}$) is

$$c_{c,L} u_L H_L = Q_* L \qquad \text{(A-52)}$$

With an equation of state to relate $c_{c,L}$ and ρ_L, Equation (A-51) is integrated from the upwind edge of the source ($x = x_{up}$) to the downwind edge ($x = L + x_{up}$).

In order to generate the initial conditions for the downwind dispersion calculations, the maximum concentration c_c and the vertical dispersion parameter S_z are needed. Since Equations (A-51) and (A-52) are written for a vertically averaged layer, consider the vertical average of the power law distribution. The height of the layer H_L is the height to some concentration level, say 10 percent of the maximum. Although strictly a function of α, this value is modeled by

$$H_L = \delta_L H_{EFF} \tag{A-53}$$

where H_{EFF} is the effective height defined by Equation (A-79) and δ_L is 2.15. The vertically averaged concentration $c_{c,L}$ can be defined by

$$c_{c,L} H_L = \int_0^\infty c\,dz \tag{A-54}$$

And similarly, the effective transport velocity u_L is defined by

$$c_{c,L} u_L H_L = \int_0^\infty c u_x\,dz \tag{A-55}$$

With Equation (A-53) and defining relations for H_{EFF} and u_{EFF} (Equations (A-79) and (A-93), respectively), it follows that

$$c_c = \delta_L c_{c,L} \tag{A-56}$$

$$u_L H_L = \delta_L \left[\frac{u_0 z_0}{1 + \alpha} \right] \left[\frac{S_z}{z_0} \right]^{1+\alpha} \tag{A-57}$$

and

$$\delta_L w_e' = w_e \tag{A-58}$$

where w_e' is given by Equation (A-83).

4. Maximum Atmospheric Takeup Rate

The maximum atmospheric takeup rate will be the largest takeup rate which satisfies Equations (A-51) and (A-52). As well, the maximum concentration of contaminant in the power law profile at the downwind edge of the source will be the source contaminant concentration $(c_c)_s$. If Equations (A-51) and (A-52) are combined along with the assumption of adiabatic mixing of ideal gases with the same

constant molal heat capacity (i.e. $\left[\frac{\rho - \rho_a}{c_c}\right] = \gamma = \text{constant}$), the maximum takeup flux is modeled by

$$Q_{*max} = (c_c)_s \frac{ku_*(1 + \alpha)}{\bar{\phi}} \left[\frac{\delta_L}{\delta_L - 1}\right] \tag{A-59}$$

where

$$\frac{1}{\bar{\phi}} = \frac{1}{L} \int_0^L \frac{dx}{\phi} \tag{A-60}$$

An upper bound of the atmospheric takeup flux can be characterized by the condition where the source begins to spread as a gravity intrusion against the approach flow. In water flume experiments, Britter (Reference 22) measured the upstream and lateral extent of a steady state plume from a circular source as a function of Ri_*. A significant upstream spread was obtained for $Ri_* > 32$, and lateral spreading at the center of the source was insignificant for $Ri_* < 8$. The presence of any significant lateral spreading represents a lower bound on the conditions of the maximum takeup flux.

The integral of Equation (A-60) is calculated using a local Richardson number of

$$Ri_*(x) = \zeta(x - x_{up})^{\frac{1}{1+\alpha}} \tag{A-61}$$

where

$$\zeta = g\left[\frac{\rho - \rho_a}{\rho_a}\right]\frac{z_0}{u_*^2}\frac{\Gamma\left(\frac{1}{1+\alpha}\right)}{1+\alpha}\left[\frac{ku_*(1+\alpha)}{\phi_c}\left(\frac{1+\alpha}{u_0 z_0}\right)\left(\frac{\delta_L}{\delta_L - 1}\right)\right]^{\frac{1}{1+\alpha}} \tag{A-62}$$

and ϕ_c is 3.1 (corresponding to $Ri_* = 20(8 < Ri_* < 32)$). Using this $Ri_*(x)$ and the first two terms of $\phi(Ri_*)$, Equation (A-60) is

$$\frac{1}{\bar{\phi}} = \frac{1}{L}\int_0^L \frac{dx}{0.88 + 0.099\,\zeta^{1.04}\,x^{\frac{1.04}{1+\alpha}}}$$

In order to simplify the numerical problem, the integral is approximated as

$$\frac{1}{\bar{\phi}} = \frac{1}{0.099\,L\,\zeta^{1.04}}\ln\left[\frac{0.88 + 0.099\,\zeta^{1.04}\,L^{\left(\frac{1.04}{1+\alpha}\right)}}{0.88}\right] \tag{A-63}$$

which then specifies the maximum atmospheric takeup flux.

5. Transient HTAG Release Simulation

If a steady state spill is being simulated, the transient source calculation is carried out until the source characteristics are no longer varying significantly with time. The maximum centerline concentration c_c, the horizontal and vertical dispersion parameters S_y and S_z, the half-width, b, and if necessary, the enthalpy, h, are used as initial conditions for the downwind calculation specified in a transient spill.

If a transient spill is being simulated, the spill is modeled as a series of pseudo-steady-state releases. Consider a series of observers traveling with the wind over the transient gas source described above; each observer originates from the point which corresponds with the maximum upwind extent of the gas blanket

($x = -R_{max}$). The desired observer velocity is the average transport velocity of the gas u_{EFF} from Equation (A-93); however, the value of u_{EFF} will differ from observer to observer with the consequence that some observers may be overtaken by others. For a neutrally buoyant cloud, u_{EFF} becomes a function of downwind distance alone which circumvents this problem. With this functionality, Colenbrander (Reference 17) models the observer velocity as

$$u_i(x) = \frac{u_0}{\Gamma\left(\frac{1}{1+\alpha}\right)} \left(\frac{S_{z_{0m}}}{z_0} \right)^{\alpha} \left[\frac{x + R_{max}}{\frac{\sqrt{\pi}}{2} R_m + R_{max}} \right]^{\alpha/(1+\alpha)} \qquad \text{(A-64)}$$

where $S_{z_{0m}}$ is the value of S_{z_0} when the averaged source rate ($\pi R^2 Q_*$) is a maximum and the subscript i denotes Observer i. Noting that $u_i(x) = dx_i/dt$, observer position and velocity as functions of time are determined.

A pseudo-steady-state approximation of the transient source is obtained as each observer passes over the source. If t_{up_i} and t_{dn_i} denote the times when Observer i encounters the upwind and downwind edges of the source respectively, then the source fetch seen by Observer i is:

$$L_i = x_{up_i} - x_{dn_i} \qquad \text{(A-65)}$$

The width of the source $2B_i'(t)$ is defined by

$$B_i'^2(t) = R^2(t) - x_i^2(t) \qquad \text{(A-66)}$$

Then the gas source area seen by Observer i is

$$2L_i b_i = 2 \int_{t_{up_i}}^{t_{dn_i}} B_i' u_i \, dt \qquad \text{(A-67)}$$

where $2b_i$ is the average width.

The takeup rate of contaminant $(Q_* Lb)_i$ is calculated as

$$2(Q_* Lb)_i = 2 \int_{t_{up_i}}^{t_{dn_i}} Q_* B_i' u_i dt \qquad \text{(A-68)}$$

The total mass flux rate from the source is

$$2(\rho_L u_L H_L b)_i = 2 \int_{t_{up_i}}^{t_{dn_i}} \left(\rho_a w_e' + \left(\frac{Q_*}{w_c} \right) \right) B_i' u_i dt \qquad \text{(A-69)}$$

With these equations, the average composition of the layer can be determined at each $x = x_{up}$ over the source. With the enthalpy of the layer given by

$$(h_L \rho_L u_L H_L b)_i = \int_{t_{up_i}}^{t_{dn_i}} h \left(\frac{Q_*}{w_c} \right) B_i' u_i dt \qquad \text{(A-70)}$$

due to the choice of the reference temperature as the ambient temperature along with a suitable equation of state relating enthalpy, temperature, and density, the source can be averaged for each observer. After the average composition of the layer is determined at the downwind edge, an adiabatic mixing calculation is performed between this gas and the ambient air when applicable. This calculation represents the function between density and concentration for the remainder of the calculation if the calculation is adiabatic; it represents the adiabatic mixing condition if heat transfer is included in the downwind calculation.

For each of several observers released successively from $x = -R_{max}$, the observed dimensions L and b, the downwind edge of the source x_{dn}, the average vertical dispersion coefficient S_z, the average takeup flux Q_*, the centerline concentration c_c, and if applicable, the average enthalpy h_L can be determined for each observer. With these input values, a steady state calculation is made for each observer. The distribution parameters for any specified time t_s are determined by locating the position of the

series of observers at time t_s, i.e. $x_i(t_s)$. The corresponding concentration distribution is then computed from the assumed profiles.

B. STEADY-STATE DOWNWIND DISPERSION

The model treats dispersion of gas entrained into the wind field from an idealized rectangularly shaped source of width 2b and length L. The circular source cloud is represented as an equivalent area square ($L^2 = \pi R^2 = 2bL$). Similarity forms for the concentration profiles are assumed which represent the plume as being composed of a horizontally homogeneous section in which only vertical dispersion is considered, with Gaussian concentration profile edges as follows:

$$c(x,y,z) = c_c(x) \exp\left[- \left(\frac{|y| - b(x)}{S_y(x)} \right)^2 - \left(\frac{z}{S_z(x)} \right)^{1+\alpha} \right] \qquad \text{for } |y| > b$$

$$= c_c(x) \exp\left[- \left(\frac{z}{S_z(x)} \right)^{1+\alpha} \right] \qquad \text{for } |y| \le b \tag{A-71}$$

A power law wind velocity profile is assumed

$$u_x = u_0 \left(\frac{z}{z_0} \right)^{\alpha} \tag{A-72}$$

where the value of α is determined by a weighted least squares fit of the logarithmic profile

$$u_x = \frac{u_*}{k} \left[\ln \left(\frac{z + z_R}{z_R} \right) - \Psi \left(\frac{z}{\lambda} \right) \right] \tag{A-73}$$

Functional forms for Ψ and typical values of α are given in Table A-1 for different Pasquill stability categories. With these

TABLE A-1. TYPICAL ATMOSPHERIC BOUNDARY LAYER STABILITY AND WIND PROFILE CONCENTRATIONS

Pasquill Stability Category	Monin-Obukhov Length (λ) as a Function of Surface Roughness z_R(m)[1]	Typical Power Law Exponents α in Eq. (A-72)	Corrections to Logarithmic Profiles as Given by Businger et al. (Reference 32) ψ in Eq. (A-73)
A	$-11.4\ z_R^{0.10}$	0.108	$\psi = 2\ln\left[\frac{1+a}{2}\right] + \ln\left[\frac{1+a^2}{2}\right] - 2\tan^{-1}(a) + \frac{\pi}{a}$, with $a = (1-15(z/\lambda))^{1/4}$
B	$-26.0\ z_R^{0.17}$	0.112	
C	$-123\ z_R^{0.30}$	0.120	
D	∞	0.142	$\psi = 0$
E	$123\ z_R^{0.30}$	0.203	$\psi = -4.7(z/\lambda)$
F	$26.0\ z_R^{0.17}$	0.253	

[1] Curve fit of data from Pasquill (Reference 31).

profiles, the parameters of Equation (A-71) are constrained by ordinary differential equations.

1. Vertical Dispersion

The vertical dispersion parameter S_z is determined by requiring that it satisfy the diffusion equation

$$u_x \frac{\partial c}{\partial x} = \frac{\partial}{\partial z} K_z \frac{\partial c}{\partial z} \tag{A-74}$$

with the vertical turbulent diffusivity given by

$$K_z = \frac{k u_* z}{\phi(Ri_*)} \tag{A-75}$$

The function $\phi(Ri_*)$ is a curve fit of laboratory scale data for vertical mixing in stably-density-stratified fluid flows reported by McQuaid (Reference 21), Kantha et al. (Reference 29), and Lofquist (Reference 20) for $Ri_* > 0$. For $Ri_* < 0$, the function $\phi(Ri_*)$ is taken from Colenbrander and Puttock (Reference 18) and has been modified so the passive limit of the two functions agree as follows:

$$\begin{aligned} \phi(Ri_*) &= 0.88 + 0.099\ Ri_*^{1.04} + 1.4 \times 10^{-25}\ Ri_*^{5.7} && Ri_* \geq 0 \\ &= 0.88/(1 + 0.65\ |Ri_*|^{0.6}) && Ri_* < 0 \end{aligned} \tag{A-76}$$

The friction velocity is calculated using Equation (A-73) from a known velocity u_0 at a specific height z_0. Combining the assumed similarity forms for concentration and velocity, Equations (A-71), (A-72), (A-74), and (A-75) give

$$\frac{d}{dx}\left[\left(\frac{u_0 z_0}{1+\alpha}\right)\left(\frac{S_z}{z_0}\right)^{1+\alpha}\right] = \frac{k u_* (1+\alpha)}{\phi(Ri_*)} \tag{A-77}$$

where the Richardson number Ri_* is computed as

$$Ri_* = g\left(\frac{\rho - \rho_a}{\rho_a}\right)\frac{H_{EFF}}{u_*^2} \tag{A-78}$$

and the effective cloud depth is defined as

$$H_{EFF} = \frac{1}{c_c}\int_0^\infty c\,dz = \Gamma\left(\frac{1}{1+\alpha}\right)\frac{S_z}{1+\alpha} \tag{A-79}$$

Equation (A-77) can be viewed as a volumetric balance on a differential slice of material downwind of the source. For a mass balance over the same slice,

$$\frac{d}{dx}\left[\rho_L u_L H_L\right] = \rho_a w_e \tag{A-80}$$

which is the same result as Equation (A-51) without the source term. With Equations (A-57) and (A-58), this is

$$\frac{d}{dx}\left(\rho_L u_{EFF} H_{EFF}\right) = \rho_a w_e' \tag{A-81}$$

Using the assumption of adiabatic mixing of ideal gases with the same constant molal heat capacity (i.e. $\frac{\rho - \rho_a}{c_c}$ = constant) along with the contaminant material balance, the mass balance becomes

$$\frac{d}{dx}\left(u_{EFF} H_{EFF}\right) = w_e' \tag{A-82}$$

which leads to

$$w_e' = \frac{w_e}{\delta_L} = \frac{k u_* (1+\alpha)}{\phi(Ri_*)} \tag{A-83}$$

Equations (A-81) and (A-83) are combined to give

$$\frac{d}{dx}\left(\rho_L u_{EFF} H_{EFF}\right) = \frac{\rho_a k u_* (1+\alpha)}{\phi(Ri_*)} \tag{A-84}$$

Furthermore, Equation (A-84) is assumed to apply when $(\rho - \rho_a)/c_c$ is not constant.

When heat transfer from the surface is present, vertical mixing will be enhanced by the convective turbulence due to heat transfer. Zeman and Tennekes (Reference 33) model the resulting vertical turbulence velocity as

$$\frac{w}{u_*} = \left[1 + \frac{1}{4} \left(\frac{w_*}{u_*} \right)^2 \right]^{1/2} \tag{A-85}$$

where w_* is the convective scale velocity described as

$$\left(\frac{w_*}{u_*} \right)^2 = \left[\frac{gh}{u_* \bar{u}} \frac{\left(T_s - T_{c,L} \right)}{T_{c,L}} \right]^{2/3} \tag{A-86}$$

If $\bar{u}$ is evaluated at H_{EFF},

$$\frac{w}{u_*} = \left[1 + \frac{1}{4} Ri_T^{2/3} \right]^{1/2} \tag{A-87}$$

where

$$Ri_T = g \left(\frac{T_s - T_{c,L}}{T_{c,L}} \right) \frac{H_{EFF}}{u_* u_0} \left(\frac{z_0}{H_{EFF}} \right)^{\alpha} \tag{A-88}$$

and $T_{c,L}$ is the temperature obtained from the energy balance of Equations (A-102) and (A-103). Equation (A-84) is modified to account for this enhanced mixing by

$$\frac{d}{dx} \left[\rho_L u_{EFF} H_{EFF} \right] = \frac{\rho_a k w (1 + \alpha)}{\phi(Ri'_*)} \tag{A-89}$$

where $Ri'_* = Ri_* \left(\frac{u_*}{w} \right)^2$.

Although derived for two-dimensional dispersion, this is extended for application to a HTAG plume which spreads laterally as a density intrusion:

$$\frac{d}{dx}\left[\rho_L u_{EFF} H_{EFF} B_{EFF}\right] = \frac{\rho_a kw(1+\alpha)}{\phi(Ri'_*)} B_{EFF} \qquad \text{(A-90)}$$

where the plume effective half width is defined by

$$B_{EFF} = b + \frac{\sqrt{\pi}}{2} S_y \qquad \text{(A-91)}$$

and determined using the gravity intrusion relation

$$\frac{dB_{EFF}}{dt} = C_E \left[g \left(\frac{\rho - \rho_a}{\rho_a} \right) H_{EFF} \right]^{1/2} \qquad \text{(A-92)}$$

The average transport velocity in the plume is defined by

$$u_{EFF} = \frac{\int_0^\infty c u_x dz}{\int_0^\infty c dz} = u_0 \left(\frac{S_z}{z_0} \right)^\alpha \Big/ \Gamma\left(\frac{1}{1+\alpha} \right) \qquad \text{(A-93)}$$

and the lateral spread of the cloud is modeled by

$$\frac{dB_{EFF}}{dx} = \frac{1}{u_{EFF}} \frac{dB_{EFF}}{dt}$$

$$= C_E \left[\frac{g z_0 \Gamma^3\left(\frac{1}{1+\alpha}\right)}{u_0^2 (1+\alpha)} \right]^{1/2} \left[\frac{\rho - \rho_a}{\rho_a} \right]^{1/2} \left(\frac{S_z}{z_0} \right)^{\left(\frac{1}{2} - \alpha\right)} \qquad \text{(A-94)}$$

2. Horizontal Dispersion

The crosswind similarity parameter $S_y(x)$ is also determined by requiring that it satisfy the diffusion equation

$$u_x \frac{\partial c}{\partial x} = \frac{\partial}{\partial y} \left[K_y \frac{\partial c}{\partial y} \right] \qquad \text{(A-95)}$$

with the horizontal turbulent diffusivity given by

$$K_y = K_0 u_x B_{EFF}^{\gamma_1} \tag{A-96}$$

When b = 0, $S_y = \sqrt{2}\ \sigma_y$, where σ_y is the similarity parameter correlated by Pasquill (Reference 31) in the form $\sigma_y = \delta x^{\beta}$. Furthermore, Equations (A-95) and (A-96) require that

$$\sigma_y \frac{d\sigma_y}{dx} = K_0 B_{EFF}^{\gamma_1} \tag{A-97}$$

where $\gamma_1 = 2 - 1/\beta$ and $K_0 = \frac{2\beta}{\pi} (\delta\sqrt{\pi/2})^{1/\beta}$. Then

$$S_y \frac{dS_y}{dx} = \frac{4\beta}{\pi} B_{EFF}^2 \left[\frac{\delta\sqrt{\pi/2}}{B_{EFF}} \right]^{1/\beta} \tag{A-98}$$

where Equation (A-98) is also assumed applicable for determining S_y when b is not zero.

At the downwind distance x_t where b = 0, the crosswind concentration profile is assumed Gaussian with S_y given by

$$S_y = \sqrt{2}\ \delta(x + x_p)^{\beta} \tag{A-99}$$

where x_v is a virtual source distance determined as

$$S_y(x_t) = \sqrt{2}\ \delta(x_t + x_p)^{\beta} \tag{A-100}$$

The gravity spreading calculation is terminated for $x > x_t$.

For a steady plume, the centerline concentration c_c is determined from the material balance

$$E = \int_0^{\infty} \int_{-\infty}^{\infty} c u_x dy dz = 2 c_c \left(\frac{u_0 z_0}{1 + \alpha} \right) \left(\frac{S_z}{z_0} \right)^{1+\alpha} B_{EFF} \tag{A-101}$$

where E is the plume source strength.

3. Energy Balance

For some simulations of cryogenic gas releases, heat transfer to the plume in the downwind dispersion calculation may be important, particularly in low wind conditions. The source calculation determines a gas/air mixture initial condition for the downwind dispersion problem. Air entrained into the plume is assumed to mix adiabatically. Heat transfer to the plume downwind of the source adds additional heat. This added heat per unit mass D_h is determined by an energy balance on a uniform cross section as

$$\frac{d}{dx}\left[D_h \rho_L u_{EFF} H_{EFF} \right] = q_s/\delta_L \qquad \text{(A-102)}$$

where q_s is determined by Equation (A-37) along with the desired method of calculating h_0. Equation (A-102) is applied when $b = 0$ and is extended to

$$\frac{d}{dx}\left[D_h \rho_L u_{EFF} H_{EFF} B_{EFF} \right] = q_s \, B_{EFF} \, / \, \delta_L \qquad \text{(A-103)}$$

when $b > 0$. Since the average density of the layer ρ_L cannot be determined until the temperature (i.e. D_h) is known, a trial and error procedure is required.

Equations (A-77), (A-78), (A-79), (A-87)-(A-91), (A-94), and (A-98)-(A-103) are combined with an equation of state relating cloud density to gas concentration and temperature and are solved simultaneously to predict S_z, S_y, c_c, and b as functions of downwind distance beginning at the downwind edge of the gas source.

C. CORRECTION FOR ALONG-WIND DISPERSION

Following Colenbrander (Reference 17), an adjustment to the values of c_c is applied to account for dispersion parallel to the wind direction. The calculated centerline concentration $c_c(x)$ is considered to have resulted from the release of successive planar puffs of gas ($c_c(x)\Delta x$) without any dispersion in the x-direction. If it is assumed that each puff diffuses in the x-direction as the

puff moves downwind independently of any other puff and that the dispersion is one-dimensional and Gaussian, the x-direction concentration dependence is given by

$$c_c'(x,x_{p_i}) = \frac{c_c(x_{p_i})\Delta x_i}{\sqrt{2\pi}\,\sigma_x} \exp\left[-\frac{1}{2}\left[\frac{x - x_{p_i}}{\sigma_x}\right]^2 \right] \qquad \text{(A-104)}$$

where x_{p_i} denotes the position of the puff center due to observer i.

After Beals (Reference 34), the x-direction dispersion coefficient σ_x is assumed to be a function of distance from the downwind edge of the gas source ($X = x - x_0$) and atmospheric stability given by

$$\begin{aligned} \sigma_x(X) &= 0.02\,X^{1.22} && \text{unstable, } x \geq 130 \text{ m} \\ &= 0.04\,X^{1.14} && \text{neutral, } x \geq 100 \text{ m} \\ &= 0.17\,X^{0.97} && \text{stable, } x \geq 50 \text{ m} \end{aligned} \qquad \text{(A-105)}$$

where ($X = x - x_0$) and σ_x are in meters. The concentration at x is then determined by superposition, i.e., the contribution to c_c at a given x from neighboring puffs is added to given an x-direction corrected value of c_c'. For N observers,

$$c_c'(x) = \sum_{i=1}^{N} \frac{c_c(x_{p_i})}{\sqrt{2\pi}\,\sigma_x} \exp\left[-\frac{1}{2}\left[\frac{x - x_{p_i}}{\sigma_x}\right]^2 \right] \Delta x_i \qquad \text{(A-106)}$$

and for large N,

$$c_c'(x) = \frac{1}{\sqrt{2\pi}} \int_0^{\infty} \frac{c_c(\xi)}{\sigma_x(\xi - \xi_0)} \exp\left[-\frac{1}{2}\left[\frac{x - \xi}{\sigma_x(\xi - \xi_0)}\right]^2 \right] d\xi \qquad \text{(A-107)}$$

The corrected centerline concentration c_c' is used in the assumed profiles in place of c_c, along with the distribution parameters S_y, S_z, and b.

D. DEGADIS MODEL INPUTS AND OUTPUTS

As implemented under VAX/VMS*, DEGADIS requires three areas of input information:

-- VAX/VMS command procedure for execution
-- simulation definition
-- numerical parameters

The VAX/VMS command procedure used to execute DEGADIS is generated in DEGADISIN by default. As well, DEGADISIN is the interactive input module which generates the simulation definition from user responses. An example input session is included in Section 3. The numerical parameters (convergence criteria, initial increments, etc.) are supplied to DEGADIS through a series of input files. Although these numerical parameters are easily changed, the user should need to change these only rarely with the exception of the time sort parameters. Additional information can be found in Reference 3.

1. VAX/VMS Command Procedure

The VAX/VMS command procedure generated by DEGADISIN controls the execution of images for the simulation. Image execution follows one of two paths, either for a transient release or for a steady state release. DEGADISIN will automatically generate the appropriate command procedure. DEGADISIN requires a simulation name be specified. The simulation name must be a valid VAX/VMS file name without a file extension and is designated herein as RUNNAME. DEGADIS will use

---

*VAX and VMS are registered trademarks of Digital Equipment Corporation.

this file name with standard extensions for input, interprocess communication, and output.

2. Simulation Definition

DEGADISIN is an interactive method of simulation definition where the user specifies information about the ambient wind field, the properties of the released gas, and some details of the release. A summary of required input information is included in Figure A-5.

The ambient wind field is characterized by a known velocity u_0 at a given height z_0, a surface roughness z_R, and the Pasquill stability class. The Pasquill stability class is used to estimate values of the lateral similarity parameter coefficients δ and β (Reference 31), values of the along-wind similarity coefficients (Reference 34), and the Monin-Obukhov length λ used by Businger et al. (Reference 32) in their logarithmic velocity profile function. The Monin-Obukhov length is then used to calculate the friction velocity u_*. Once these parameters have been estimated using the Pasquill stability class, the user has the option of interactively changing any of these to better describe the simulation. In addition to these specifications, the ambient temperature, pressure, and humidity must be specified.

The properties of air and the released gas are used to evaluate the mixture density as a function of temperature and composition. The desired released gas properties include the molecular weight MW_c, the storage temperature (normal boiling point for cryogenic gases) T_0, the vapor phase density at the storage temperature and ambient pressure ρ_0, and two constants q_1 and p_1 which describe the heat capacity according to the equation

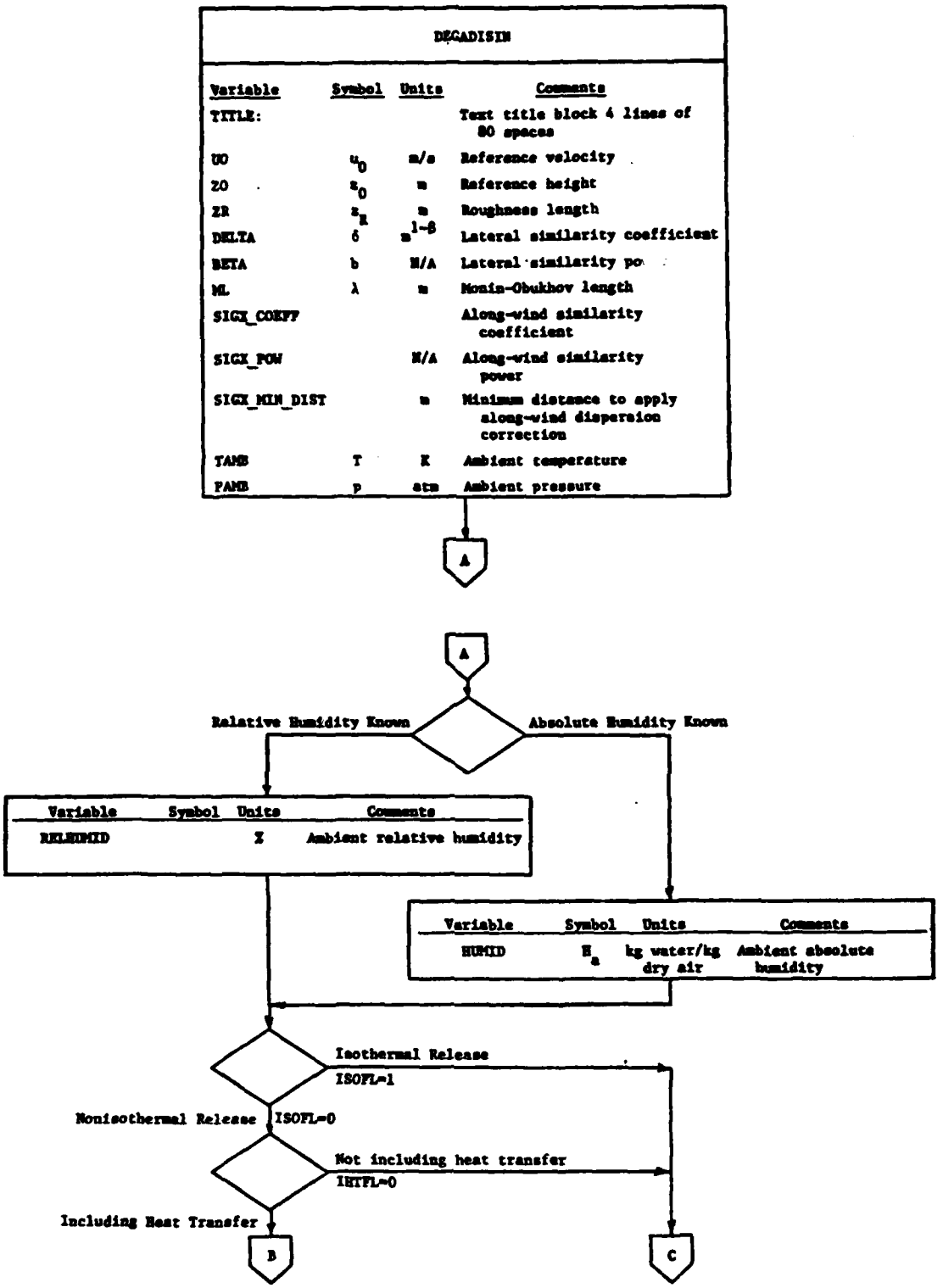

Figure A-5. Summary of simulation definition input information for DEGADIS.

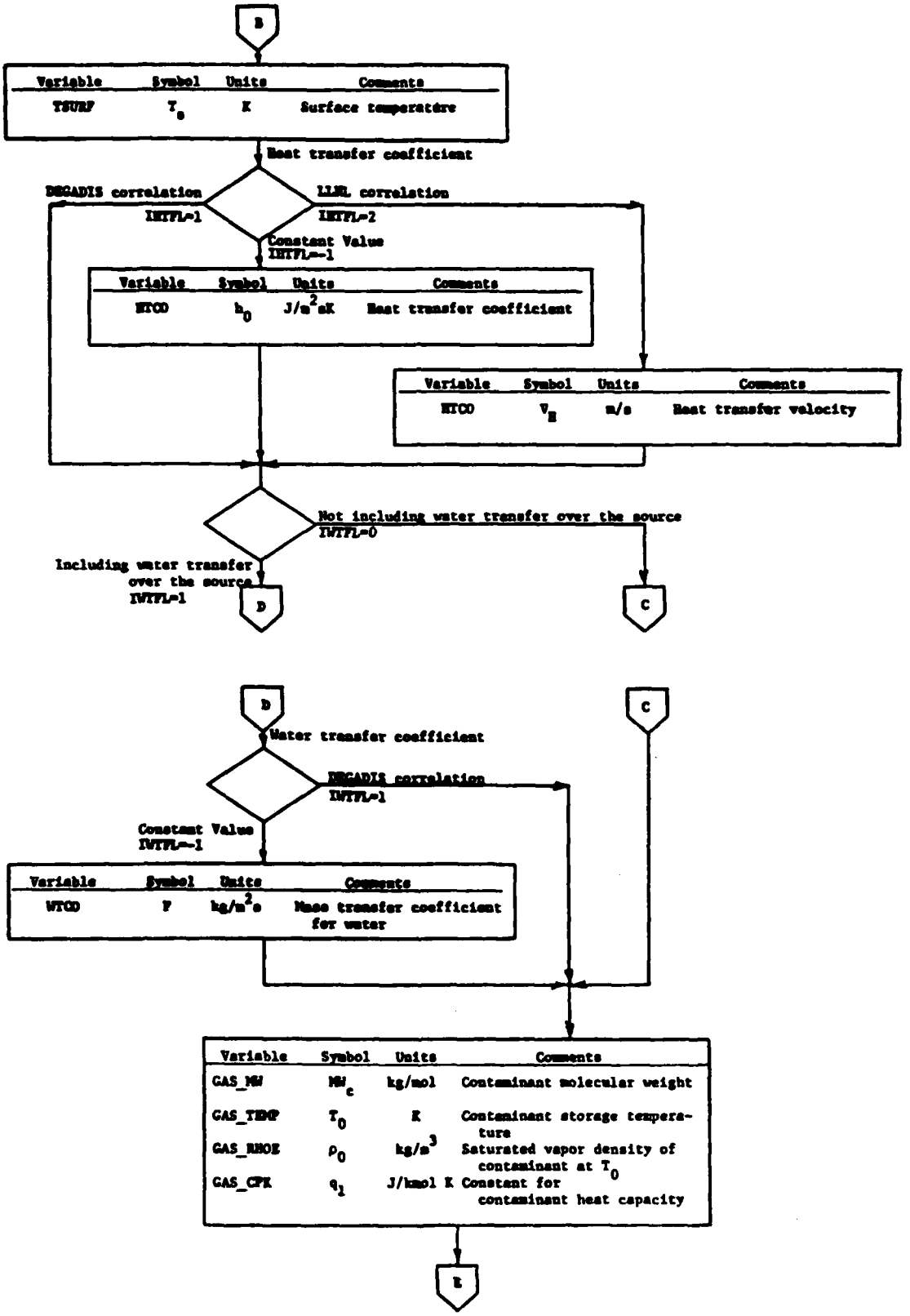

Figure A-5. (continued)

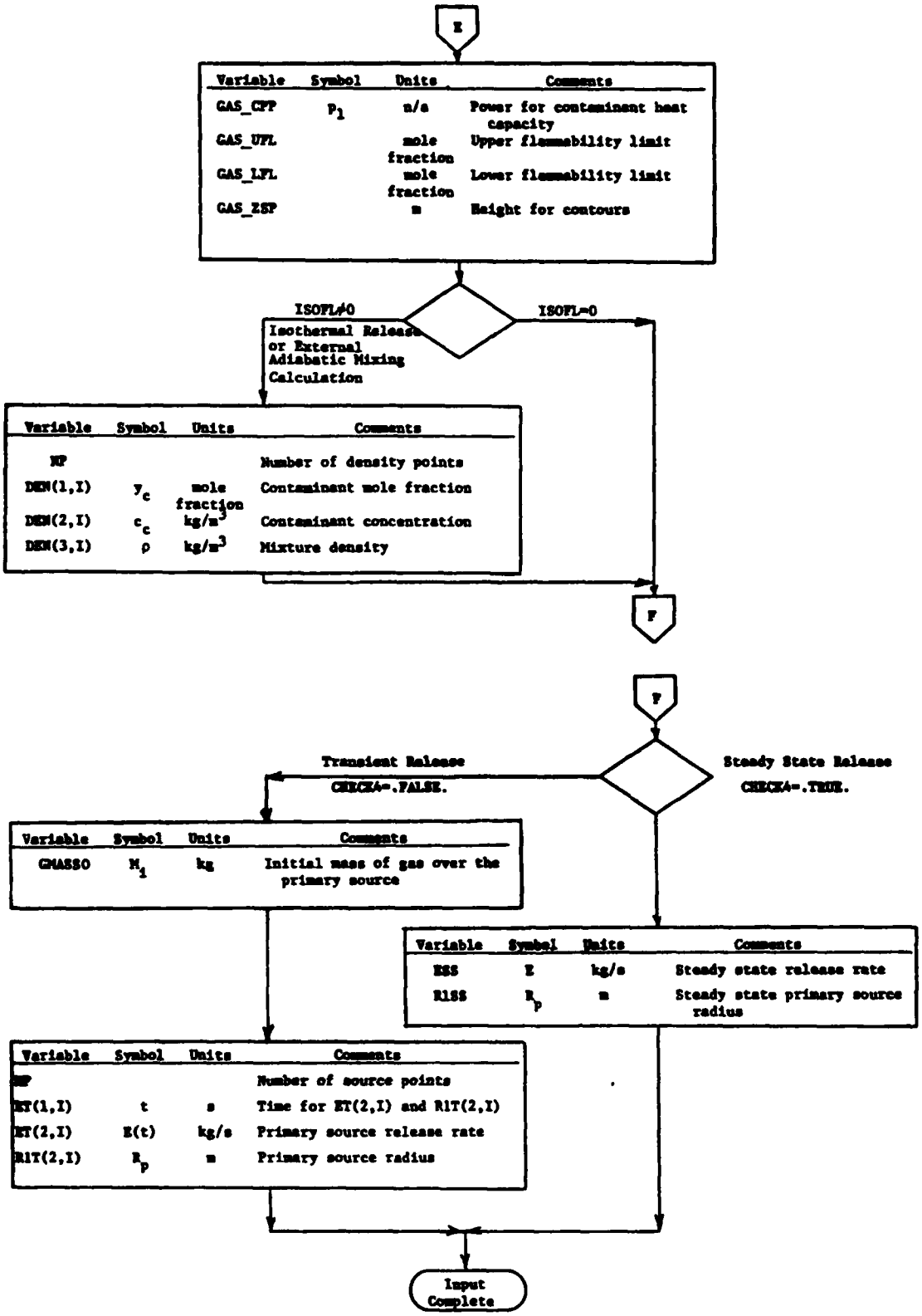

Figure A-5. (continued)

$$C_{p_c}(T) = (MW_c)^{-1}\left[3.33 \times 10^4 + q_1\left[\frac{T^{p_1} - T_0^{p_1}}{T - T_0}\right]\right] \quad \text{(A-108)}$$

where $C_{p_c}(T)$ is the mean heat capacity (J/kg K) at temperature T. Note that a constant heat capacity with respect to temperature can be obtained by setting $p_1 = 1.0$ and choosing the appropriate value for q_1. Representative gas properties for liquefied natural gas (LNG) as methane, liquefied petroleum gas (LPG) as propane, pure unreacted NO_2, and pure unreacted N_2O_4 are included in DEGADISIN. Also included are the lower and upper flammability limits (LFL and UFL, respectively) for LNG and LPG.

The user may also choose to calculate the mixture density as a function of composition using some other method. This mixture density is entered in the program as if the release were isothermal; for each composition, the program requests the contaminant mole fraction, the contaminant concentration, and the mixture density. For ease of input, these values may be entered from a file made available to DEGADISIN.

In specifying the details of the release, the user must choose to simulate the release as transient or steady state. For both release types, the area source is assumed circular. The source radius and emission rate must be specified for a steady state release only once, while these must be specified as a function of time for transient releases (either interactively or by file). For transient releases, the user must specify the initial amount of gas present over the source (in order to simulate, for example, instantaneous releases such as the Thorney Island Trials).

Figure A-5 summarizes the simulation information gathered by DEGADISIN contained in the RUNNAME file with extension INP. The structure of RUNNAME.INP is illustrated

in Figure A-6. At this point, RUNNAME.INP may be edited to correct any misinformation entered during the input session. Note that care must be exercised when editing RUNNAME.INP due to the fact that information contained in the file can be different depending on the answered questions (e.g. steady state versus transient simulation).

```
EAGLE 6 test simulation as an ISOTHERMAL release of PURE NO2 WITHOUT
CHEMICAL REACTION using the HIGH SOURCE RATE.  The source gas is assumed to
have the same temperature as the LIQUID POOL TEMPERATURE (15C).

   5.580000        12.00000        1.0000000E-06
     4
  0.1300000       0.9000000       0.0000000E+00
  4.0000000E-02    1.140000        100.0000
   295.7500       0.9090000       6.7578776E-03
    1   295.7500
    0  0.0000000E+00
    0  0.0000000E+00
NO2
   46.00000        295.7500        1.769000
   3845.000        1.000000
  1.0000000E-03  5.0000000E-04  0.5000000
     2
  0.0000000E+00  0.0000000E+00   1.081600      0.0000000E+00   295.7500
   1.000000        1.769000        1.769000      0.0000000E+00   295.7500
  3.0000000E-04
  0.0000000E+00
     4
  0.0000000E+00   1.720000        10.00000
   6023.000        1.720000        10.00000
   6024.000       0.0000000E+00  0.0000000E+00
   6025.000       0.0000000E+00  0.0000000E+00
 F F F F T F
 9-MAY-1986 14:11:56.90
   1.720000        17.72454        17.72454
```

Figure A-6. EAGLE6.INP LISTING.

3. Example Input Sessions

The input procedures for simulation of the transient release and the steady state release are very similar. Therefore, only the specification of a steady-state release (Eagle 3) has been included. In the point-by-point discussion of the input procedure, note the following:

(*) The file name specification RUNNAME must satisfy system restrictions.

(*) A line terminator (normally a carriage return) must end every line entered by the user.

(*) When DEGADISIN requests the user to choose an option, all acceptable responses are a single character (capital or lower case). The default responses are denoted by a capital letter inside angle brackets (e.g. <N>). When applicable, a menu of acceptable responses is included inside parentheses.

(*) For numerical responses, a comma, space, tab, or line terminator (carriage return) may separate the numbers.

(*) When a file is used as input (i.e., for the density or transient source input), DEGADISIN reads the same information from the file which would be entered at the terminal in the same order and in the same format.

```
(1)   $ RUN DEGADISIN

                    DEnse GAs DISpersion Model input module.

(2)   Enter the simulation name : [DIR]RUNNAME EAGLE6
          INPUT MODULE -- DEGADIS MODEL

          **********************************
(3)       Enter Title Block -- up to 4 lines of 80 characters
          To stop, type "//"
      EAGLE 6 test simulation as an ISOTHERMAL release of PURE NO2 WITHOUT
      CHEMICAL REACTION using the HIGH SOURCE RATE.  The source gas is assumed to
      have the same temperature as the LIQUID POOL TEMPERATURE (15C).
      //

(4)       ENTER WIND PARAMETERS -- U0 (m/s), Z0 (m), and ZR(m)
          U0 -- Wind velocity at reference heisht Z0
          ZR -- Surface Roughness
      5.58,12.00,1.E-6

(5)       Enter the Pasquill stability class: (A,B,C,D,E,F) <D>

(6)   The values for the atmospheric parameters are set as follows:
      DELTA:                          0.1300
      BETA:                           0.9000

(7)   Monin-Obukhov length:      infinite
      Sigma X Coefficient:            0.0400
      Sigma X Power:                  1.1400
      Sigma X Minimum Distance:     100.0000 m
      Do you wish to change any of these?
      (No,Delta,Beta,Length,Coefficient,Power,Minimum) <N>

(8)   Enter the ambient temperature(C) and pressure(atm): 22.6,.909

      The ambient humidity can be entered as Relative or Absolute.
      Enter either R or A <R or a>:
      Enter the relative humidity (%): 35.

(9)   Ambient Air density is    1.0816     kg/m**3
```

NOTES ON STEADY-STATE SIMULATION OF EAGLE6

(1) Begin the input procedure by execution of DEGADISIN.

(2) The file name specification must follow system restrictions. The DEGADIS model uses this file name along with various file extensions for input and output.

(3) The Title Block is used to carry any desired comments such as information on the specification of certain parameters.

(4) The wind field parameters include the wind velocity (m/s) at a specified height (m) and the surface roughness (m).

(5) The Pasquill stability class is used to generate estimates of other atmospheric parameters which follow.

(6) The current settings of pertinent atmospheric parameters are displayed in this list. If any of these are to be changed, the first letter of the parameter to be changed is entered. Note that the default--indicated by <N>--is No for no changes.

(7) The value of the Monin-Obukhov length is indicated to be infinite (which is the default value for a Pasquill D stability). Any value of the Monin-Obukhov length can be specified, but an infinite value is a special case which can be obtained for any Pasquill stability class by setting the Monin-Obukhov length to 0.

(8) The ambient temperature and pressure are entered.

(9) DEGADISIN calculates the ambient air density for the given input parameters.

(10) Is this an Isothermal spill? <y or N> Y

(11) Enter the code name of the diffusing species: NO2

(12) The characteristics for the gas are set as follows:

Molecular weight:	46.00
Storage temperature [K]:	295.75
Density at storage temperature, PAMB [kg/m**3]:	1.7231
Mean Heat capacity constant	3845.0
Mean Heat capacity power	1.0000
Upper Flammability Limit [mole frac]	1.00000E-03
Lower Flammability Limit [mole frac]	5.00000E-04
Height of Flammability Limit [m]	0.50000

Do you wish to change any of these? (No,Mole,Temp,Den,Heat,Power,Upper,Lower,Z) <N> D
Enter the desired Density at Storage Temperature and ambient pressure: 1.769

(13) The characteristics for the gas are set as follows:

Molecular weight:	46.00
Storage temperature [K]:	295.75
Density at storage temperature, PAMB [kg/m**3]:	1.7690
Mean Heat capacity constant	3845.0
Mean Heat capacity power	1.0000
Upper Flammability Limit [mole frac]	1.00000E-03
Lower Flammability Limit [mole frac]	5.00000E-04
Height of Flammability Limit [m]	0.50000

Do you wish to change any of these? (No,Mole,Temp,Den,Heat,Power,Upper,Lower,Z) <N>

(14) The density is determined as a function of concentration
by a listing of ordered triples supplied by the user.
Use the following form:

```
first point      -- pure air  y=0.0,Cc=0.,RHOG=RHOA=   1.0816     kg/m**3
     .
     .
     .
last point       -- pure gas  y=1.0,Cc=RHOE,RHOG=RHOE
```

(10) If the release is isothermal, respond "Y". A positive response causes DEGADISIN to ask for a list of concentration, density, and mole fraction points for the gas mixture. The default response is negative. For the Eagle series, the simulations were made as though the releases were isothermal. Although the releases were not isothermal, the difference in temperature between the liquid pool and the ambient air were considered small enough to be negligible. A sample DEGADIS input session for LNG can be found in Reference 3.

(11) Enter the three-letter designation of the diffusing gas. The properties of LNG as methane, LPG as propane, pure NO_2 (without reaction), and pure N_2O_4 (without reaction) are included.

(12) A list of the properties for the specified gas (if available) is given. If any of the parameters are to be changed, the first letter of the parameter to be changed in the list is given to the prompt. Here, the vapor density at the storage temperature is changed. Note that for NO_2 (and N_2O_4), the storage temperature is assumed to be the ambient temperature, and the vapor density is calculated by the ideal gas equation of state. For this simulation, it was unnecessary to change the storage temperature since heat transfer was not included although the new vapor density value is calculated from the liquid pool temperature.

(13) The gas property list is displayed again. The default response is no change.

(14) Since this is an isothermal simulation, the density and concentration must be specified as a function of mole fraction.

(15) Do you have an input file for the Density function? [y or N]

ENTER THE NUMBER OF DATA TRIPLES (max=30) FOR THE DENSITY FUNCTION: 2

Enter Mole frac, Cc (kg/m**3), then RHOG (kg/m**3) by triples
0.,0.,1.0816
1.,1.769,1.769

(16) The suggested LOWEST CONCENTRATION OF INTEREST (gas_lfl/2.)
is 4.42250E-04 kg/m**3. Enter the desired value: 3.0E-4

Specification of source rate and extent.

(17) Is this a Steady state simulation? <y or N> Y

Enter the desired evolution rate [=] kg/sec : 1.72
Enter the desired source radius [=] m : 10.

(18) In addition to the information just obtained, DEGADIS
requires a series of numerical parameter files which use
the same name as [DIR]RUNNAME given above.

For convenience, example parameter files are included for
each step. They are:
EXAMPLE.ER1 and
EXAMPLE.ER2
Note that each of these files can be edited during the course of the
simulation if a parameter proves to be out of specification.

(19) Do you want a command file to be generated to execute the procedure? <Y or n>
The command file will be generated under the file name:
EAGLE6.com

(20) Do you wish to initiate this procedure? <y or N>
$

(15) A file may be used to enter the density information. In the file, the first line should have the number of data triples. Each subsequent line should contain a mole fraction, concentration, and density for the gas mixture.

(16) The lowest concentration of interest is the concentration at which the calculations are stopped.

(17) If a steady state release is to be simulated, type "Y" to the prompt. For a steady simulation, the steady state mass evolution rate (kg/s) and primary source extent (m) are required.

(18) A note about the numerical parameter files is included. These files contain various constant values used in the programs to which the user has access without recompiling the programs. Access is granted as a convenience.

(19) DEGADISIN will generate a command procedure suitable for running the model under VMS.

(20) If so desired, DEGADISIN will initiate the command procedure under VMS. If not, the program returns to the operating system.

The generated INP file for EAGLE6 is shown in Figure A-6. If necessary, the user may edit the INP file before beginning the simulation.

4. Example Simulation Output

After proper completion of the model, EAGLE6.LIS contains the output listing for the steady state releases. Following is a point-by-point discussion of the output.

UOA_DEGADIS MODEL OUTPUT -- VERSION 1.3

********** ********** 9-MAY-1986 14:54:06.79 ***

(1)

Data input on 9-MAY-1986 14:11:56.90
Source program run on 9-MAY-1986 14:54:06.79

```
*************************************************************************
*
*       NOTE:
*       -----
*
*       >    All Calculations are limited to circular liquid sources.
*
*************************************************************************
```

TITLE BLOCK

(2)

EAGLE 6 test simulation as an ISOTHERMAL release of PURE NO2 WITHOUT CHEMICAL REACTION using the HIGH SOURCE RATE. The source gas is assumed to have the same temperature as the LIQUID POOL TEMPERATURE (15C).

Wind velocity at reference height		5.58	m/s
Reference height		12.00	m
Surface roughness length		1.000E-06	m
Pasquill Stability class		D	
Monin-Obukhov length		infinite	
Gaussian distribution constants	Delta	0.13000	m
	Beta	0.90000	
Wind velocity power law constant	Alpha	0.06869	
Friction velocity		0.11981	m/s
Ambient Temperature		295.75	K
Ambient Pressure		0.909	atm
Ambient Absolute Humidity		6.758E-03	kg/kg BDA
Ambient Relative Humidity		35.00	%

(1) The date and time DEGADISIN was run is included.

(2) The input information gathered by DEGADISIN is repeated to assist in documentation of the simulations. Included here are the Title Block and the atmospheric conditions.

(3) Input:

Mole fraction	CONCENTRATION OF C ks/m**3	GAS DENSITY ks/m**3
0.00000	0.00000	1.08160
1.00000	1.76900	1.76900

Specified Gas Properties:

Molecular weight:	46.000	
Storage temperature:	295.75	K
Density at storage temperature and ambient pressure:	1.7690	ks/m**3
Mean heat capacity constant:	3845.0	
Mean heat capacity power:	1.0000	
Upper mole fraction contour:	1.00000E-03	
Lower mole fraction contour:	5.00000E-04	
Height for isopleths:	0.50000	m

(4) Source input data points

Initial mass in cloud: 0.00000E+00

TIME s	SOURCE STRENGTH ks/s	SOURCE RADIUS m
0.00000E+00	1.7200	10.000
6023.0	1.7200	10.000
6024.0	0.00000E+00	0.00000E+00
6025.0	0.00000E+00	0.00000E+00

(5) Calculation procedure for ALPHA: 1

Entrainment prescription for PHI: 3

Layer thickness ratio used for average depth: 2.1500

Air entrainment coefficient used: 0.590

Gravity slumping velocity coefficient used: 1.150

Isothermal calculation

Heat transfer not included

Water transfer not included

(3) Continuing with the input information, the contaminant gas properties are output.

(4) The specification of the mass evolution rate and source radius are output. For a steady-state release, there is no initial mass in the cloud, and the source strength and source radius are held constant for an arbitrarily large period of time.

(5) Finally, certain numerical parameters and calculation flags are displayed. Some of these are set in DEGADISIN while others are set in the numerical parameter files.

⑥

***** CALCULATED SOURCE PARAMETERS *****

Time s	Gas Radius m	Height m	Ostar kg/m**2/s	SZ(x=L/2.) m	Mole frac C	Density kg/m**3	Rich No.
60.2300	10.0000	0.000000E+00	5.474930E-03	0.197496	4.713647E-02	1.11323	0.000000E+00
301.150	10.0000	0.000000E+00	5.474930E-03	0.197496	4.713647E-02	1.11323	0.000000E+00

⑦

Source strength [kg/s] : 1.7200 Equivalent Primary source radius [m] : 10.000

Equivalent Primary source length [m] : 17.725 Equivalent Primary source width [m] : 17.725

Secondary source concentration [kg/m**3] : 8.14073E-02 Secondary source SZ [m] : 0.19750

Contaminant flux rate: 5.47493E-03

Secondary source mass fractions... contaminant: 7.312693E-02 air: 0.92065

Enthalpy: 0.00000E+00 Density: 1.1132

Secondary source length [m] : 17.725 Secondary source half-width [m] : 8.8623

(6) A summary of the calculated secondary source parameters is included. The secondary source gas radius and height are output as functions of time along with other secondary parameters including the source mass flux (Qstar), the vertical concentration distribution parameter at the downwind edge (SZ(x = L/2.)), the contaminant mole fraction (Mole frac C), the gas mixture density (Density), and the Richardson number based on the cloud spreading velocity (Rich No.).

(7) For a steady-state release, the source calculations are terminated after the calculated parameters are no longer changing as a function of time. A summary of the steady-state secondary source is included.

(8)

Distance (m)	Mole Fraction	Concentration (kg/m**3)	Density (kg/m**3)	Temperature (K)	Half Width (m)	Sz (m)	Sy (m)	Width to 5.000E-02moleZ at z= (m)	Width 0.100 moleZ 0.50 m (m)
8.26	4.714E-02	8.141E-02	1.13	296.	8.86	0.197	5.33	16.1	14.5
10.1	4.473E-02	7.724E-02	1.11	296.	8.64	0.206	5.67	16.4	14.9
11.3	4.253E-02	7.345E-02	1.11	296.	8.44	0.215	5.99	16.8	15.2
13.7	3.868E-02	6.680E-02	1.11	296.	8.06	0.233	6.59	17.5	15.8
15.3	3.645E-02	6.293E-02	1.11	296.	7.81	0.245	6.97	18.0	16.1
18.5	3.268E-02	5.641E-02	1.10	296.	7.20	0.271	7.66	18.6	16.7
21.7	2.959E-02	5.108E-02	1.10	296.	6.63	0.297	8.30	19.3	17.2
28.1	2.489E-02	4.296E-02	1.10	296.	5.61	0.350	9.45	20.3	18.0
34.5	2.146E-02	3.703E-02	1.10	296.	4.71	0.402	10.5	21.2	18.7
47.3	1.682E-02	2.902E-02	1.09	296.	3.12	0.505	12.3	22.5	19.6
60.1	1.381E-02	2.382E-02	1.09	296.	1.73	0.607	13.8	23.5	20.2
72.9	1.170E-02	2.019E-02	1.09	296.	0.490	0.709	15.2	24.3	20.6
85.7	1.015E-02	1.752E-02	1.09	296.	0.000E+00	0.809	15.8	24.4	20.5
89.1	9.757E-03	1.684E-02	1.09	296.	0.000E+00	0.828	16.0	24.6	20.7
90.5	9.383E-03	1.619E-02	1.09	296.	0.000E+00	0.847	16.3	24.9	20.9
95.3	8.695E-03	1.500E-02	1.09	296.	0.000E+00	0.885	16.7	25.3	21.1
98.5	8.277E-03	1.428E-02	1.09	296.	0.000E+00	0.911	17.1	25.6	21.3
105.	7.525E-03	1.298E-02	1.09	296.	0.000E+00	0.962	17.7	26.2	21.7
111.	6.869E-03	1.185E-02	1.09	296.	0.000E+00	1.01	18.3	26.7	21.9
124.	5.787E-03	9.985E-03	1.09	296.	0.000E+00	1.12	19.6	27.7	22.4
137.	4.939E-03	8.522E-03	1.08	296.	0.000E+00	1.22	20.9	28.6	22.7

AD-A172 856 DEVELOPMENT OF VAPOR DISPERSION MODELS FOR NONNEUTRALLY BUOYANT GAS MIXTU..(U) ARKANSAS UNIV FAYETTEVILLE DEPT OF CHEMICAL ENGINEERING T O SPICER ET AL. SEP 86 2/2

UNCLASSIFIED AFESC/ESL-TR-86-24 DTCG23-80-C-2029 F/G 4/1 NL

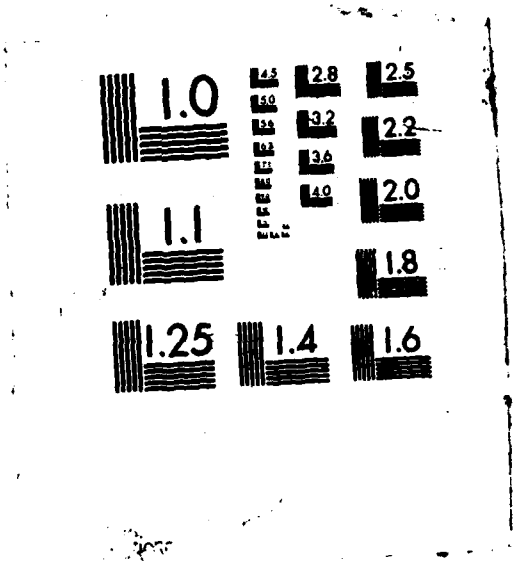
1.0
1.1
1.25
1.4
1.6
1.8
2.0
2.2
2.5
2.8
3.2
3.6
4.0
4.5
5.0
5.6

(8) The downwind portion of the calculation is included. The distance downwind of the source is given in the first column. Columns 2 through 5 contain the mole fraction, contaminant concentration, mixture density, and mixture temperature on the centerline of the gas cloud at ground level. Columns 6 through 8 contain the contour shape parameters b (Half Width), S_z, and S_y. Finally, columns 9 and 10 contain the width from the centerline to the indicated concentration levels at the indicated height. Note that the output is prematurely terminated. Output actually continues until the centerline, ground-level concentration drops below the lowest concentration of interest.

4. Model Limitations and Cautions

DEGADIS model application should be limited to the description of atmospheric dispersion of heavier-than-air gas releases at ground level onto flat, unobstructed terrain or water. Application to releases from sources above ground level (e.g. overflow from dikes) would be expected to give conservative predictions of the downwind hazard zones, but this has not been verified.

The dispersion of a heavier-than-air gas by the action of the wind assumes the maintenance of a wind velocity profile in the gas cloud or plume whose characteristics are determined by the approach wind flow (upwind of the release). The treatment of vertical momentum transfer invokes the assumption of a logarithmic vertical velocity profile, which is in turn curve-fitted to a power law vertical velocity profile. DEGADIS also uses similarity forms for the vertical profile of gas concentration in the cloud, and the vertical profile is dependent on the power law exponent α used in the representation of the velocity profile. The vertical velocity profile, which is directly related to the air entrainment velocity into the cloud, is dependent on the factors which determine the structure of the atmospheric boundary surface layer, wind speed, surface roughness, and atmospheric stability. Consequently, the representations of the vertical velocity and concentration profiles in DEGADIS are subject to similar limitations as in other descriptions of the surface layer. Table A-2 indicates typical recommended surface roughness values. Table A-1 indicates logarithmic wind velocity profile corrections for different atmospheric stabilities, along with typical values of the wind profile power law exponent α determined in DEGADIS.

TABLE A-2. TYPICAL VALUES OF SURFACE ROUGHNESS

Terrain	z_R (m)
Mud flats, ice	10^{-5}
Calm, open sea	10^{-4}
Off-sea wind in coastal areas	10^{-3}
Cut grass (~ 3 cm)	0.007
Long grass (~ 60 cm), crops	0.04

Demonstration of the model has been primarily directed to the prediction of hazard extent defined by gas concentrations in the hydrocarbon flammable limit range (~1 to 20 percent). Based on the simulations of field experiments presented in Reference 3, the ratio of observed distance to calculated distance for a given time-averaged concentration level (OBS/PRE) ranged from 0.73 to 0.96 for the 5 percent level nine out of ten times (i.e. 90 percent confidence interval). For the 2.5 percent level, (OBS/PRE) ranged from 0.82 to 1.03 for a 90 percent confidence interval. For the 1 percent level, (OBS/PRE) ranged from 0.95 to 1.24 for a 90 percent confidence interval. If for a given release scenario the calculated distance to the 2.5 percent average concentration level was 120 m, the distance to the 2.5 percent average concentration for nine out of ten realizations of the same release would be expected to range between 98 m and 124 m.

REFERENCES

1. McRae, T. G., "Analysis and Model/Data Comparisons of Large-Scale Releases of Nitrogen Tetroxide," Lawrence Livermore National Laboratories Report UCID-20388, June 1985.

2. McRae, T. G., R. T. Cederwell, H. C. Goldwire, Jr., D. L. Hipple, G. W. Johnson, R. P. Koopman, J. W. McClure, and L. K. Morris, "Eagle Series Data Report: 1983 Nitrogen Tetroxide Spills," Lawrence Livermore National Laboratories Report UCID-20063, June 1984.

3. Havens, J. A. and T. O. Spicer, "Development of an Atmospheric Dispersion Model for Heavier-than-Air Gas Mixtures," Final Report to U.S. Coast Guard, CG-D-23-80, USCG HQ, Washington, DC, May 1985.

4. Stretch, D. D., R. E. Britter, and J. C. R. Hunt, "The Dispersion of Slightly Dense Contaminants," in Atmospheric Dispersion of Heavy Gases and Small Particles, G. Ooms and H. Tennekes, eds., Springer-Verlag, Berlin, 1984.

5. Conner, A. Z., F. E. DeVry, M. Plunguian, H. M. Spurlin, R. B. Wagner, and C. M. Wright, Nitrogen Tetroxide, Hercules Incorporated, Wilmington, Delaware, 1968.

6. Verhoek, F. H. and F. Daniels, "The Dissociation Constants of Nitrogen Tetroxide and of Nitrogen Tetroxide," Journal of the American Chemical Society, 53, 1931.

7. Giaque, W. F. and J. D. Kemp, "The Entropies of Nitrogen Tetroxide and Nitrogen Dioxide. The Heat Capacity from 15°K to the Boiling Point. The Heat of Vaporization and Vapor Pressure. The Equilibrium $N_2O_4 = 2NO_2 = 2NO + O_2$," Journal of Chemical Physics, 6, 1938.

8. Nordstrom, R. J. and W. H. Chan, "A Spectroscopic Study of the NO_2 - N_2O_4 System by the Infrared Absorption Technique," Journal of Physical Chemistry, 80, 1976.

9. Dean, J. A., (ed.), Lange's Handbook of Chemistry, McGraw-Hill, New York, 1985.

10. England, C. and W. H. Corcoran, "Kinetics and Mechanisms of the Gas Phase Reaction of Water Vapor and Nitrogen Dioxide," Industrial Engineering Chemistry, Fundamentals, 13, 1984.

11. Goyer, G. G., "The Formation of Nitric Acid Mists," Colloid Science, 18, 1963.

12. McHaney, L. R. J., "The Vapor Phase Reactions between Nitrogen Oxides and Water," Master of Science Thesis, University of Illinois, Urbana, Illinois, 1953.

13. Burdick, C. L., "The Oxidation of Nitric Oxide and Its Catalysts," Journal of the American Chemical Society, 44, 1922.

14. Hilbers, C. E., "Titan II Toxic Sources," BSD TR 65-97, February 1963 (available through DTIC as AD361799).

15. Haugen, D. A. and J. J. Fuquay, "The Ocean Breeze and Dry Gulch Diffusion Programs," AFCFL-63-791, 1963.

16. Hanna, S. R., G. A. Briggs, and R. P. Hosker, "Handbook on Atmospheric Dispersion," DOT/TC-11223, 1982.

17. Colenbrander, G. W., "A Mathematical Model for the Transient Behavior of Dense Vapor Clouds," 3rd International Symposium on Loss Prevention and Safety Promotion in the Process Industries, Basel, Switzerland, 1980.

18. Colenbrander, G. W. and J. S. Puttock, "Dense Gas Dispersion Behavior: Experimental Observations and Model Developments," International Symposium on Loss Prevention and Safety Promotion in the Process Industries, Harrogate, England, 1983.

19. Kantha, L. H., O. M. Phillips, and R. S. Azad, "On Turbulent Entrainment at a Stable Density Interface," Journal of Fluid Mechanics, 79, 1977.

20. Lofquist, Karl, "Flow and Stress Near an Interface Between Sratified Liquids," Physics of Fluids, 3, 1960.

21. McQuaid, James, "Some Experiments on the Structure of Stably Stratified Shear Flows," Technical Paper P21, Safety in Minds Research Establishment, Sheffield, UK, 1976.

22. Britter, R. E., "The Ground Level Extent of a Negatively Buoyant Plume in a Turbulent Boundary Layer," Atmospheric Environment, 14, 1980.

23. van Ulden, A. P., "A New Bulk Model for Dense Gas Dispersion: Two-Dimensional Spread in Still Air," I.U.T.A.M. Symposium on Atmospheric Dispersion of Heavy Gases and Small Particles, Delft University of Technology, The Netherlands, August 29-September 2, 1983.

24. Batchelor, G. K., An Introduction to Fluid Dynamics, Cambridge University Press, Cambridge, UK, 1967.

25. van Ulden, A. P., "The Unsteady Gravity Spread of a Dense Cloud in a Calm Environment," 10th International Technical Meeting on Air Pollution Modeling and its Applications," NATO-CCMS, Rome, Italy, October, 1979.

26. Simpson, J. E. and R. E. Britter, "The Dynamics of the Head of a Gravity Current Advancing over a Horizontal Surface," Journal of Fluid Mechanics, 94, Part 3, 1979.

27. Koopman, R_3 P. et al., "Description and Analysis of Burro Series 40m^3 LNG Spill Experiments," Lawrence Livermore National Laboratories Report UCRL-53186, August 14, 1981.

28. McAdams, W. H., Heat Transmission, McGraw-Hill, New York, 1954.

29. Treybal, R. E., Mass Transfer Operations, 3rd edition, McGraw-Hill, New York, 1980.

30. Bird, R. B., W. E. Stewart, and E. N. Lightfoot, Transport Phenomena, John Wiley & Sons, Inc. Publishers, New York, 1960.

31. Pasquill, F., Atmospheric Dispersion, 2nd edition, Halstead Press, New York, 1974.

32. Businger, J. A., J. C. Wyngaard, Y. Izumi, and E. F. Bradley, "Flux-Profile Relationships in the Atmospheric Surface Layer," Journal of the Atmospheric Sciences, 28, March 1971.

33. Zeman, O. and H. Tennekes, "Parameterization of the Turbulent Energy Budget at the Top of the Daytime Atmospheric Boundary Layer," Journal of the Atmospheric Sciences, January 1977.

34. Beals, G. A., "A Guide to Local Dispersion of Air Pollutants," Air Weather Service Technical Report 214, April 1971.

(The reverse of this page is blank.)

END

10-86

DTIC